

DR CÉSAR LLAVE (Orcid ID : 0000-0003-3844-4582)

Article type : MS - Regular Manuscript

The immune repressor BIR1 contributes to antiviral defense and undergoes transcriptional and post-transcriptional regulation during viral infections

Irene Guzmán-Benito^{1,2}, Livia Donaire¹, Vítor Amorim-Silva³, José G. Vallarino³, Alicia Esteban³, Andrzej T. Wierzbicki⁴, Virginia Ruiz-Ferrer¹, César Llave¹

¹Departamento de Biotecnología Microbiana y de Plantas, Centro de Investigaciones Biológicas, CSIC, 28040-Madrid, Spain; ²Doctorado en Biotecnología y Recursos Genéticos de Plantas y Microorganismos Asociados, ETSI Agronómica, Alimentaria y de Biosistemas, Universidad Politécnica de Madrid, 28040-Madrid, Spain; ³Departamento de Biología Molecular y Bioquímica, Instituto de Hortofruticultura Subtropical y Mediterránea ‘‘La Mayora’’, Universidad de Málaga-CSIC (IHSM-UMA-CSIC), Universidad de Málaga, Campus Teatinos, 29071-Málaga, Spain; ⁴Department of Molecular, Cellular, and Developmental Biology, University of Michigan, Ann Arbor, MI 48109, USA

Author for correspondence: César Llave

E-mail: cesarllave@cib.csic.es

Phone: +34-91-8373112

Received: 2 April 2019

Accepted: 15 May 2019

This is the author manuscript accepted for publication and has undergone full peer review but has not been through the copyediting, typesetting, pagination and proofreading process, which may lead to differences between this version and the [Version of Record](#). Please cite this article as doi: [10.1111/NPH.15931](https://doi.org/10.1111/NPH.15931)

This article is protected by copyright. All rights reserved

ORCID information

Irene Guzmán-Benito	0000-0002-9912-8164
Livia Donaire	0000-0002-5454-2994
Vitor Amorim-Silva	0000-0002-3978-7205
José G. Vallarino	0000-0002-0374-8706
Alicia Esteban	0000-0003-3039-1172
Andrzej T. Wierzbicki	0000-0002-5713-1306
Virginia Ruiz-Ferrer	0000-0002-7840-297X
César Llave	0000-0003-3844-4582

Summary

- BIR1 is a receptor-like kinase that functions as a negative regulator of basal immunity and cell death in *Arabidopsis*.
- Using *Arabidopsis thaliana* and *Tobacco rattle virus* (TRV), we investigate the antiviral role of BIR1, the molecular mechanisms of *BIR1* gene expression regulation during viral infections, and the effects of BIR1 overexpression on plant immunity and development.
- We found that SA acts as a signal molecule for *BIR1* activation during infection. Inactivating mutations of BIR1 cause strong antiviral resistance that is not due to constitutive cell death or SA defense priming in the *bir1-1* mutant. RNA-directed DNA methylation (RdDM) and post-transcriptional silencing are both required to negatively regulate *BIR1* expression upon viral induction. *BIR1* overexpression causes severe developmental defects, cell death and premature death that correlate with the constitutive activation of plant immune responses.
- Our findings suggest that BIR1 acts as a negative regulator of antiviral defense in plants, and indicate that RNA silencing contributes, alone or in conjunction with other regulatory mechanisms, to define a threshold expression for proper BIR1 function beyond which an autoimmune response may occur. This work provides novel mechanistic insights into the regulation of *BIR1* homeostasis that may be common for other plant immune components.

Key words

Antiviral defense, BAK1, BIR1, plant innate immunity, plant viruses, post-transcriptional silencing, RNA-directed DNA methylation, SOBIR1

Introduction

To defend themselves against invaders, plants have evolved potent inducible immune responses (Dangl & Jones, 2001). The frontline of active defense relies on the recognition of conserved microbial components named Pathogen-Associated Molecular Patterns (PAMPs) by membrane-localized receptor-like kinases (RLK) and receptor-like proteins (RLP) to induce PAMP-Triggered Immunity (PTI) (Boller & Felix, 2009; Tena *et al.*, 2011). PTI prevents colonization by pathogens such as bacteria, fungi and oomycetes and includes activation of mitogen-activated protein kinases (MAPK), production of reactive oxygen species (ROS), generation of the signal molecule salicylic acid (SA), differential expression of genes, callose deposition and stomatal closure (Dodds & Rathjen, 2010). Pathogens hit back by producing effectors that suppress different steps of PTI, resulting in Effector-Triggered Susceptibility (ETS) (Jones & Dangl, 2006). As a counter-counter defense strategy, plants possess a repertoire of polymorphic disease resistance (R) proteins containing nucleotide-binding (NB) and leucine-rich repeat (LRR) domains (Martin *et al.*, 2003; Meyers *et al.*, 2003). These R immune receptors can sense effectors directly or indirectly and establish Effector-Triggered-Immunity (ETI). ETI responses significantly overlap with PTI signaling cascades, albeit with a stronger amplitude, and often result in a form of programmed cell death at the infection sites that restricts pathogen progression (Coll *et al.*, 2011).

Recent studies show that RNA silencing is a key regulatory checkpoint modulating both PTI and ETI responses in plants (Zvereva & Pooggin, 2012; Boccara *et al.*, 2014). Growing evidence illustrates the role of PAMP-responsive microRNAs (miRNAs) and small interfering RNAs (siRNAs) in plant innate immunity against microbial pathogens (Katiyar-Agarwal *et al.*, 2006; Navarro *et al.*, 2006; Katiyar-Agarwal *et al.*, 2007; Navarro *et al.*, 2008; Li *et al.*, 2010; Zhang *et al.*, 2011; Campo *et al.*, 2013; Boccara *et al.*, 2014; Li *et al.*, 2014; Ouyang *et al.*, 2014), and it is well documented how small RNA regulatory networks exert extensive post-transcriptional control of disease resistance genes to prevent undesirable R-mediated autoimmunity in unchallenged plants (Yi & Richards, 2007; Zhai *et al.*, 2011;

Boccaro *et al.*, 2014). Furthermore, RNA-directed DNA methylation (RdDM) provides epigenetic control of plant defenses by targeting transposable elements and their adjacent defense genes (Downen *et al.*, 2012; Yu *et al.*, 2013; Lopez Sanchez *et al.*, 2016). Immune responses against viruses are thought to rely mostly on ETI upon recognition of virus-specific effectors by intracellular immune-R receptors (Zvereva & Pooggin, 2012). In this line, interesting connections between RNA silencing-mediated regulation of R genes and viral infections have been made. For instance, Brassica miR1885 is induced specifically by *Turnip mosaic virus* (TuMV) infection, and targets NB-LRR class disease-resistant transcripts for cleavage (He *et al.*, 2008). Also, members of the miR482/2118 superfamily mediate silencing of multiple NB-LRR disease resistance genes in tomato, which includes production of RNA-dependent RNA polymerase 6 (RDR6)-dependent secondary siRNAs (Shivaprasad *et al.*, 2012). Interestingly, the miR482-mediated silencing cascade is suppressed in plants infected with viruses or bacteria allowing pathogen-inducible expression of NB-LRR targets (Shivaprasad *et al.*, 2012). In another study, two miRNAs (miR6019 and miR6020) guide cleavage and production of functional secondary siRNAs from transcripts of the NB-LRR immune receptor *N* from tobacco that confers resistance to *Tobacco mosaic virus* (TMV) (Li *et al.*, 2012). Overexpression of both miRNAs attenuates *N*-mediated resistance to TMV, demonstrating that miRNAs and secondary siRNAs have a functional role in regulating resistance to TMV.

Although in plants, apparently, there are no equivalent PAMPs derived from viruses, several studies have suggested a role of PTI in antiviral defense (Korner *et al.*, 2013; Gouveia *et al.*, 2016; Nicaise & Candresse, 2017). For instance, a recent report shows that Arabidopsis mutants deficient in the PTI master regulator *BRASSINOSTEROID INSENSITIVE1 (BRI1)-ASSOCIATED RECEPTOR KINASE1 (BAK1)* exhibit increased susceptibility to different RNA viruses (Korner *et al.*, 2013). BAK1 interacts *in vivo* with the RLK BAK1-INTERACTING RECEPTOR-LIKE KINASE 1 (BIR1), a negative regulator of PTI responses and cell death pathways in Arabidopsis (Gao *et al.*, 2009). It has been suggested that BIR1 sequesters BAK1 to prevent unwanted interactions with ligand-binding receptors in the absence of pathogens (Gao *et al.*, 2009; Ma *et al.*, 2017). Here, we study the role of BIR1 during viral infections and the molecular mechanisms whereby *BIR1* is regulated. We further show that *BIR1* regulation is critical to avoid constitutive activation of plant defense responses, which drastically impairs plant fitness and growth.

Materials and Methods

Plant material

Nicotiana benthamiana and *Arabidopsis thaliana* plants were grown in controlled environmental chambers under long day conditions (16h day/8h night) at 25°C and 22°C, respectively. *Arabidopsis* lines used in this study were derived from the Columbia-0 (Col-0) ecotype. Mutants for *bir1-1* and *sobir1-12* and *bir1-1/BIR1* lines were donated by Yuelin Zhang (University of British Columbia, Canada). The *Arabidopsis ago1-27*, *ago1-25*, *ago2-1* and mutant combinations involving the alleles *rdr1-1*, *rdr2-1*, *rdr6-15*, *dcl2-1*, *dcl3-1* and *dcl4-2* were donated by James C. Carrington (The Donald Danforth Plant Center, MO, USA). *Arabidopsis* mutant *cmt3* and *ddc* were supplied by Steve Jacobsen (UCLA-HHMI, USA). The *Arabidopsis nrpe1 (nrpd1b-11)* was donated by Craig Pikaard (Indiana University, USA). The *Arabidopsis* mutant *drm2-2* was supplied by Eric Richards (Boyce Thompson Institute, Cornell University, USA). The *Arabidopsis npr1-1* and NPR1ox seeds were supplied by Xinni Dong (Duke University, NC, USA).

Construction of a recombinant TRV-BIR1 vector and viral inoculation

Tobacco rattle virus (TRV) derivatives were created from an infectious TRV clone (Liu *et al.*, 2002). TRV-GFP contained the soluble modified green fluorescence protein (GFP) under the promoter region of the *Pea early browning virus* (PEBV) replicase (Fernandez-Calvino *et al.*, 2016a). TRV-BIR1 contained the *Arabidopsis BIR1* coding region under the PEBV promoter. Briefly, the *BIR1* cDNA containing its 5' UTR was amplified by RT-PCR, cloned into the Gateway pDONR207 vector, and shuffled into the binary destination vector pGWB14. The HA-tagged *BIR1* sequence was then PCR amplified, and cloned into pTRV2. The recombinant clones were screened by restriction enzyme digestion and sequencing. TuMV-GFP derived from an infectious clone of TuMV strain UK1 (Lellis *et al.*, 2002). All primers used in this study are listed in Table S1.

N. benthamiana plants were inoculated at approximately 21 days after germination by infiltration of agrocultures containing TRV or TuMV (Johansen & Carrington, 2001; Liu *et al.*, 2002). Three-week olds *Arabidopsis* plants were inoculated using sap extracts from virus-infected *N. benthamiana* leaves as described (Fernandez-Calvino *et al.*, 2014). *Arabidopsis* plants inoculated with sap from non-infiltrated *N. benthamiana* were used as controls (mock). Additionally, experiments were paralleled using naïve *Arabidopsis* plants to discard potential

side effects due to wounding caused by abrasion used during mechanical inoculation of sap extracts.

Construction of *BIR1* transgenic plants

Arabidopsis Col-0 transgenic plants expressing the GFP:GUS dual reporter gene under the *BIR1* promoter were generated using the Gateway compatible pBGWFS7 binary vector. A genomic DNA fragment of 3,297 bp containing the *BIR1* promoter was cloned upstream to the fusion reporter gene as described (Xiao *et al.*, 2010). Arabidopsis Col-0 transgenic plants expressing *BIR1* were obtained using a glucocorticoid (DEX)-inducible gene expression system (Marques-Bueno *et al.*, 2016). Briefly, the GVG::ter::6xUAS/pDONR221 contained the GVG cassette cloned into pDONR221. mCherry was added to this vector to generate GVG::ter::6xUAS::mCherry/ pDONR221. pDONR221-BIR1 contained the full-length *BIR1* protein coding gene as described above. Final destination vectors were obtained by three-fragment recombination using the pH7m34GW destination vector. All the constructs were transformed into wild type Col-0 plants according to standard floral dipping (Clough & Bent, 1998). Independent homozygous lines harboring a single transgene insertion were selected in T4 and used for subsequent experiments.

Methylation analyses

Chop-PCR was carried out as described (Bohmdorfer *et al.*, 2014) using genomic DNA (100 ng) from 3-week-old Arabidopsis rosette leaves and the methylation-sensitive restriction enzymes *DdeI* and *NlaIII*. Chop qPCR was done using Maxima Hot Start Taq DNA Polymerase (Thermo Scientific) and 25x SYBR Green (Invitrogen) diluted at 1:400.

Bisulfite sequencing was done as described (He *et al.*, 2009). Briefly, genomic DNA from 3-week-old rosette leaves was extracted using DNeasy Plant Mini Kit (QIAGEN). Bisulfite conversion was done using EZ DNA Methylation Startup kit (Zymo Research). PCR was done using Maxima Hot Start Taq DNA Polymerase (Thermo Scientific), and amplification products were cloned into TOPO TA plasmids (Invitrogen). At least 30 clones per sample were sequenced. A non-methylated region at coordinates 19,573,407 to 19,573,671 in chromosome 4 was included as bisulfite conversion control. Primers for bisulfite were designed as described (Patterson *et al.*, 2011) and listed in Table S1.

RNA analysis

Total RNA was extracted with TRIzol reagent (Invitrogen). One-step qRT-PCR was carried out using Brilliant III Ultra-Fast SYBR Green QRT-PCR Master Mix (Agilent Technologies) in a Rotor-Gene 6000/Rotor-Gene Q real-time PCR machine (Corbett/Qiagen) (Fernandez-Calvino *et al.*, 2016a). Relative gene expression was determined using the Delta-delta cycle threshold method and Rotor-Gene 6000 Series Software (Corbett). Constitutively expressed *CBP20* (*At5g44200*) or *Actin2* (*At3g18780*) transcripts were used for normalization because of its similar level of expression in mock-inoculated and virus-infected leaves. A standard curve of known concentration of *in vitro* synthesized TRV transcripts was used to determine the TRV concentration as the number of viral copies per nanogram of total RNA (Fernandez-Calvino *et al.*, 2016a). Significant differences between two or among several samples were compared by t-student test or one-way analysis of variance (ANOVA) followed by Duncan's test, respectively, using Statgraphics Plus, version 5.1 (Statistical Graphics Corp.). Unless otherwise indicated, each Arabidopsis sample used for qRT-PCR analysis consisted in RNA extracted from a pool of rosette leaves from five plants (three leaves per plant, all leaves at identical positions).

Protein analysis

Protein extracts were prepared and analyzed by immunoblot assay after SDS-PAGE (Fernandez-Calvino *et al.*, 2016b). Blotted proteins were detected using commercial horseradish peroxidase (HRP)-conjugated secondary antibodies and a chemiluminescent substrate (LiteAbiot Plus). Relative protein accumulation was measured by densitometry of protein blots exposed to autoradiographic films using the Image J Software.

Small RNA sequencing, construction of degradome libraries and 5' RACE

Young rosette leaves from virus-infected plants and the corresponding mock-inoculated plants were pooled (10-12 plants) at 8 dpi (TRV) or 14 dpi (TuMV), and used for degradome or sRNA sequencing. Systemically infected inflorescences from TRV-infected or mock-inoculated Arabidopsis were pooled (10-15 plants) at 16 dpi, and used for degradome sequencing. Total RNA was extracted using TRIzol reagent (Invitrogen) or Plant RNeasy Kit

(QIAGEN) and tested through Agilent 2100 bioanalyzer system to guarantee RNA quality. sRNA libraries were prepared and sequenced on an Illumina Genome Analyzer (HiSeq2000, 1x50bp, single-end run) by Ascidea Computational Biology Solutions (www.ascidea.com).

Parallel analysis of RNA ends (PARE) degradome libraries were done as described (German *et al.*, 2009) and sequenced on an Illumina Genome Analyzer (HiSeq2000, 1x50bp, single-end run) by Fasteris (www.fasteris.com) and IGA technology (www.igatechnology.com). Sequencing data was then analyzed using CleaveLand4 (Addo-Quaye *et al.*, 2009). Briefly, all degradome sequence reads with exact matches to structural RNA were removed and filtered dataset was mapped against the Arabidopsis cDNA sequence transcriptome (TAIR10) using Bowtie. For each exact match, 13-nt long sequences upstream and downstream of the location of the 5'-end of the matching degradome sequence was extracted to create a 26-nt long 'query' mRNA subsequence. Query sequences were then aligned to each sRNA sequence in our sRNA datasets or to miRNA reported in miRBase using GStar (Addo-Quaye *et al.*, 2009). A modified 5'-RACE was used for mapping internal cleavage sites as described (Donaire *et al.*, 2011).

SA application and determination of SA content

Three-week old plants grown on soil were sprayed with SA (1 mM) as described (Takahashi *et al.*, 2007). To test the effect of SA on TRV accumulation, plants were TRV- or mock-inoculated 24h after the first SA application and then plants were treated for eight consecutive days by spraying the solution once at intervals of 24h (Exp #1) or 48h (Exp #2). To assess SA content in the plant tissue, rosette leaves were harvested at the same leaf position in order to minimize variations in the hormone content throughout the plant. SA was extracted and derivatized as described (Vallarino & Osorio, 2016). The samples were analyzed by using gas chromatography coupled to time-of-flight mass spectrometry (GC-TOF-MS) (Pegasus III, Leco), and quantified using an internal standard ($[^2\text{H}_4]$ -SA; OlChemIm Ltd, Olomouc, Czech Republic).

Accession numbers

DNA methylation data (GSE39901) were used from (Stroud *et al.*, 2013). Degradome sequencing data from naïve Col-0 inflorescences (GSM280226) was reported previously (German *et al.*, 2008). Sequence data from this article can be found in the NCBI Gene

Expression Omnibus (GEO; <http://www.ncbi.nlm.nih.gov/geo/>) under accession numbers: GSM3019138, GSM3019139, GSM3019140 (deep sequencing of degradome tags); GSM2808011, GSM2808012, GSM3019141, GSM3019142 (deep sequencing of sRNAs).

Results

Inactivating mutations in the immune repressor BIR1 triggers resistance to TRV

To gain insight into the role of Arabidopsis *BIR1* (*At5g48380*) in the infectious process we monitored *BIR1* expression during infection with TRV in a time-course experiment. We found that *BIR1* transcripts were significantly induced in leaves of TRV-infected plants at 5 and 8 days post-inoculation (dpi) compared to mock-inoculated controls (Fig. 1a). *BIR1* was also up regulated in response to the unrelated TuMV (Fig. S1a). Using an Arabidopsis *bir1-1* mutant, we found that depletion of *BIR1* led to strong antiviral resistance against TRV (Fig. 1b). However, TRV levels were reverted back to wild type plants, or even higher, in *bir1-1* complemented lines (*bir1-1/BIR1-HA*) expressing a HA-tagged wild-type BIR1 coding gene (Fig. 1b). This result confirmed that the resistance phenotype observed in *bir1-1* was caused by mutation in *BIR1*. Western blot assay using anti-HA antibody also revealed a significant induction of BIR1 protein in *bir1-1/BIR1-HA* lines after TRV infection, indicating that elevated *BIR1* transcript levels reflected protein levels in systemically infected leaves (Fig. 1c). The *bir1-1* mutant is known to constitutively activate cell death and defense responses that are partially dependent on the SA-dependent resistance pathway (Gao *et al.*, 2009; Liu *et al.*, 2016). Accordingly, we found that transcription of the defense marker genes *PR1*, *PR4*, *PAD3* and *WRKY29* remained similarly reactivated in TRV-infected *bir1-1* mutants, indicating that virus infection does not impair the activation of defense when *BIR1* is genetically suppressed (Fig. 1d and S1b). The autoimmune phenotypes in *bir1-1* mutants are partially dependent on *SUPPRESSOR OF BIR1-1 1* (*SOBIR1*), which promotes cell death and defense in conjunction with BAK1 (Chinchilla *et al.*, 2007; Gao *et al.*, 2009; Liu *et al.*, 2016). Interestingly, we found a significant induction of *SOBIR1* transcripts in Arabidopsis leaves at early time points of TRV or TuMV infection compared to mock-inoculated plants (Fig. 1e and Fig. S1a,c). In contrast, *BAK1* transcripts decreased significantly after infection with TRV or TuMV (Fig. 1f and Fig. S1a,c). In our assay, the *bak1-5* mutant, which is strongly impaired in PTI signaling (Schwessinger *et al.*, 2011), was more susceptible to TRV accumulation (Fig. 1g), whereas TRV levels were moderately diminished in *sobir1-12* mutants (Fig. 1h). Importantly, TRV RNA levels were also drastically reduced in a *sobir1-1 bir1-1* double

mutant, in which cell death and SA-dependent defense responses are significantly reduced by the *sobir1-1* mutation (Gao *et al.*, 2009). This result suggested that TRV resistance associated to loss of *BIR1* function in the *bir1-1* mutant was unrelated to constitutive cell death or SA defense priming (Fig. 1i). Consistently with this notion, we showed that exogenous application of SA triggered accumulation of *PRI* transcripts in the plant tissue but was not sufficient to prime plant defense against TRV (Fig. 1i). Collectively, our results indicated that TRV triggers an immune response in which *BIR1* likely functions as a negative regulator of antiviral defenses.

RdDM imparts transcriptional control of *BIR1*

Inspection of Arabidopsis small RNA sequencing datasets generated in our lab revealed the profuse accumulation of siRNAs upstream of the *BIR1* transcription start site, the vast majority of which corresponded to the 24-nt class (Fig. 2a and Fig. S1d). Since 24-nt siRNAs guide methylation in the canonical RdDM pathway (Xie & Yu, 2015) we investigated if siRNA-dependent RdDM controls *BIR1* expression. First, *BIR1* transcripts were significantly more abundant in the RdDM mutants *drm2*, *drm1 drm2 cmt3* (herein *ddc*), *nrpe1* and *ago4* mutants compared to wild type plants (Fig. 2b). *BIR1* levels were unaffected in the single *cmt3* mutant, likely due to redundancy between methyltransferases *DRM2* and *CMT3* in maintaining non-CG DNA methylation (Fig. 2b) (Cao & Jacobsen, 2002). Then, we used qRT-PCR to detect RNA products at the intergenic region containing the predicted *BIR1* promoter. Interestingly, transcripts were amplified in wild type Col-0 plants but not in *nrpe1* mutants, indicating that Pol V was required for their production (Fig. 2c). The accumulation of Pol V-dependent transcripts derived from *INTERGENIC LOCUS 22* (*IGN22*) was used as a positive control (Rowley *et al.*, 2011) (Fig. S2a).

If *BIR1* were an RdDM target, DNA methylation levels at this locus should be reduced in RdDM mutants. To test this idea, we performed methylation-specific Chop-PCR to examine DNA methylation at the *BIR1* promoter region in wild type and several DNA methylation mutants. Genomic DNA was digested with the CHH methylation-sensitive restriction endonucleases *DdeI* and *NlaIII* prior to PCR amplification using flanking primers (Bohmdorfer *et al.*, 2014). We found amplification products in DNA samples treated with either *DdeI* or *NlaIII* in the wild type background, indicative of active cytosine methylation (Fig. S2b). In contrast, low levels of amplification were reported in the RdDM mutants *nrpe1*, *drm2* or *ago4* (Fig. S2b). Similar results were obtained for *At1g49490* and *IGN36*, used as

positive RdDM controls for *DdeI* and *NlaIII* digestions, respectively (Bohmdorfer *et al.*, 2014) (Fig. S2b). Parallel amplification of DNA sequences without restriction sites (*At1g55535* and *At2g36490*) from the same digested DNA samples, used as internal digestion controls, produced amplification bands in all genetic backgrounds (Fig. S2b). Quantification of the difference in DNA methylation levels by Chop-qPCR indicated that CHH methylation levels at both the *BIR1* promoter and the *At1g49490* and *IGN36* positive controls, but not the negative control, were reduced to a similar extent in all mutants tested (Fig. 2d and S2c). Finally, whole-genome bisulfite sequencing (WGBS) reported by (Wierzbicki *et al.*, 2012) revealed extensive symmetrical and asymmetrical DNA methylation in the *BIR1* promoter, whereas methylation was drastically diminished in *nrpe1* compared to wild type plants (Fig. 2a and S3). Furthermore, published Pol V RIP-seq data (Bohmdorfer *et al.*, 2016) revealed that Pol V-associated RNA accumulated in Col-0 wild type, but not in *nrpe1* mutants, confirming that RNA reads originated at the *BIR1* promoter were associated with Pol V (Fig. 2a). Collectively, our data demonstrated that *BIR1* was an RdDM target under normal growing conditions.

SA mediates transcriptional activation of *BIR1* during TRV infection

We wondered whether higher accumulation of *BIR1* transcripts in infected tissues could reflect the transcriptional activation of the *BIR1* locus in response to the virus. To test this idea, Arabidopsis plants expressing a GFP:GUS fusion protein under the control of the *BIR1* promoter were challenged with TRV. GUS activity was strongly and consistently induced in rosette leaves and aerial tissues of TRV-infected transgenic plants when compared to the mock-inoculated ones (Fig. 3a). The spatial pattern of GUS induction suggested that *BIR1* responded ubiquitously to TRV infection. Furthermore, northern blot revealed higher levels of GFP:GUS fusion transcripts in the presence of TRV confirming that TRV triggered transcriptional activation of *BIR1* (Fig. 3a).

Inspection of transcriptomic data revealed that two key SA biosynthetic genes, *ICS1* and *PAD4* (Chen *et al.*, 2009), were significantly up regulated in leaves of TRV-infected plants (Fig. 3b) (Fernandez-Calvino *et al.*, 2014). We thus wondered if SA levels influence *BIR1* expression in the infected tissue. To test this possibility, we first determined the levels of SA in the leaves of soil-grown plants using GC-TOF-MS. SA levels gradually increased from 5 to 14 dpi in TRV-infected plants, whereas they remained constant in both non-inoculated and mock-inoculated plants (Fig. 3c). We found that *BIR1* transcripts were markedly enhanced in

wild type Arabidopsis at 6 h after SA application compared to mock-treated controls (Fig. 3d). Furthermore, we observed increasing levels of GFP:GUS transcripts in Arabidopsis plants expressing a GFP:GUS reporter under the *BIR1* promoter at 6, 12 and 24 h after SA treatment, indicating that SA efficiently promotes transcriptional activation of *BIR1* (Fig. 3e). Importantly, SA-activation of *BIR1* during TRV infection was largely inhibited in the Arabidopsis *sid2-2* mutant, which has disrupted the pathogen-inducible *ICS1* gene and reduced SA accumulation (Wildermuth *et al.*, 2001) (Fig. 3f). We also found that induction of *BIR1* in virus-infected plants was compromised in *npr1-1* Arabidopsis mutants, which lack NPR1 receptor-dependent SA-signaling (Cao *et al.*, 1997; Wu *et al.*, 2012), compared to wild type or *npr1* complemented transgenic lines (OxNPR1) (Fig. 3g). These findings indicated that SA acts as a signal molecule for *BIR1* activation during TRV infection, and that TRV promotes *BIR1* expression by increasing the levels of SA in infected cells. Interestingly, TRV levels in the SA-deficient *sid2-2* mutants were lower than in wild type plants, whereas plants with the *npr1-1* mutation display enhanced susceptibility to TRV (Fig. 3h). Our results supported the idea that SA lacks direct antiviral functions against TRV, and suggest a SA-independent role for NPR1 in the control of TRV infection.

TRV activates *BIR1* without affecting its methylation status

We next asked if *BIR1* induction in infected plants was due to changes in the methylation status of its promoter. We found that siRNAs of 24 nts produced upstream of the *BIR1* transcription start were as much abundant in TRV-infected plants as in mock-inoculated controls, suggesting that epigenetic silencing of *BIR1* was not compromised by TRV (Fig. 4a). Chop-qPCR experiments revealed comparable levels of CHH methylation at the *BIR1* promoter in mock-inoculated and TRV-infected samples after digestion with *NlaIII*, whereas the relative levels of amplified DNA were slightly reduced in infected samples digested with *DdeI*, possibly due to star activity of the enzyme (Fig. 4b). No significant changes in the CHH methylation of the RdDM targets *At1g49490* and *IGN36*, used as methylation controls, were observed in plants exposed to TRV infection relative to the mock-inoculated ones (Fig. S2d). *BIR1* was induced by TRV to a similar extent in all RdDM mutants (except *drm2*), suggesting that TRV supported *BIR1* transcription regardless of its methylation status (Fig. 4c). Importantly, *BIR1* transcripts were elevated in TRV-infected *ddc*, *nrpe1* or *ago4* mutants compared to wild type plants, indicating that RdDM was important to contain *BIR1* expression during infection (Fig. 4c). Finally, similar patterns of methylation at the *BIR1*

promoter were observed in healthy, mock-inoculated and virus-infected plants when methylation was analyzed using locus-specific bisulfite sequencing (Fig. 4d and Fig. S4).

We next investigated if SA altered the DNA methylation pattern of the *BIR1* promoter. We found low levels of DNA amplification diagnostic of loss of asymmetric methylation in *nrpe1*, *drm2* or *ago4* mutants compared to wild type Col-0 plants after 6 or 12 h of SA treatment (Fig. S5a,b). DNA methylation at the *At1g49490* and *IGN36* controls diminished in RdDM mutants regardless of SA treatments (Fig. S5a). *BIR1* transcripts increased after SA treatment in wild type plants and in *nrpe1*, *drm2* or *ago4* mutants, indicating that loss of DNA methylation did not compromise SA-mediated induction of *BIR1* (Fig. S5c). Finally, transcription at the *BIR1* promoter was strongly reduced in the Pol V-defective *nrpe1* mutants in leaves of both mock-treated plants and SA-sprayed plants (Fig. S5d). Collectively, our data proved that SA activates transcription of *BIR1* during virus infections without interfering with its epigenetic regulation.

***BIR1* is regulated by post-transcriptional RNA silencing**

The analysis of our sRNA sequences revealed that siRNAs matching the *BIR1* protein-coding region were abundant in plants systemically infected with TRV or TuMV, but not in mock-inoculated ones, suggesting that *BIR1* is a target of post-transcriptional silencing during infections (Figs. 2a, 4a,e, and S1d,f). To test this possibility, we first monitored *BIR1* transcripts in non-infected Arabidopsis silencing mutants. Although data between independent repeats showed slight variations, a subtle increment of *BIR1* transcripts in some mutants involving dysfunctional DCL2, DCL3 or DCL4 as well as in mutants with genetic defects in RDR1, RDR2 or RDR6 suggested that *BIR1* may undergo conditional post-transcriptional silencing under non-challenging conditions (Fig. 5a and S6a).

When *BIR1* transcripts were measured in TRV-infected plants, we found that *BIR1* was induced in the double *dcl2 dcl3* mutants as much as the wild type (Fig. 5a). In contrast, *BIR1* transcripts were significantly more abundant in *dcl2 dcl4*, *dcl3 dcl4* or *dcl2 dcl3 dcl4* mutants compared to control plants, indicating that DCL4 was important to prevent excessive *BIR1* accumulation in the infected tissue (Fig. 5a). Similarly, *BIR1* transcripts were, in general, far more abundant in *rdr2 rdr6* and, to a lower extent, in *rdr1 rdr6* and *rdr1 rdr2 rdr6* defective mutants than in wild type infected plants (Fig. 5a). Finally, *BIR1* transcripts were similar in mock-inoculated wild type and *ago1* mutants, whereas *BIR1* transcripts were more abundant

in *ago1* when they were infected (Fig. 5a). Similar results were observed in plants systemically infected with TuMV, suggesting that post-transcriptional RNA silencing was accentuated in response to viral infections (Fig. S1e).

To support our findings, we examined *BIR1* mRNA degradation via degradome sequencing. By plotting the abundance of 5' signatures matching the *BIR1* transcript we found that TRV infection correlated with the massive accumulation of degradome 5' signatures at nucleotide positions 156, 2,219 and 2,247 (Fig. 5b). These cleavage site sequences were clearly discerned from a background of low abundant, non-specific degradation products at other positions (Fig. 5b). Cleavage at position 156 was reproducibly found with high abundance in all degradome libraries prepared from leaves or inflorescences of TRV-infected plants. Although this precise 5' signature was not found in mock-inoculated controls, degradome tags diagnostic of sequential cleavage were identified at nearby nucleotide positions in all samples tested, suggesting that this region was particularly prone to RNA degradation (Fig. 5b and S6b). When we applied the CleaveLand4 computational pipeline to match *BIR1*-derived degradome 5' signatures against the miRBase, we were unable to identify validated miRNAs as potentially responsible for cleavage at these positions, suggesting that *BIR1*-derived siRNAs may guide *cis*-cleavage events. Collectively, our data proved that *BIR1* transcripts were exposed to selective post-transcriptional degradation in response to infection.

***BIR1* overexpression causes extreme morphological defects and up regulation of plant defense in TRV-infected Arabidopsis**

To further explore the relevance of *BIR1* regulation in infected plants, we investigated the consequences of *BIR1* overexpression during TRV infection in Arabidopsis. To do this, we used TRV as a viral expression vector to overproduce *BIR1* in infected plants. We cloned a HA-tagged version of the Arabidopsis *BIR1* into pTRV2 and introduced it along with pTRV1 in *N. benthamiana* by Agrobacterium-mediated infiltration (Fig. 6a). Western blot assay using anti-HA antibody detected BIR1 protein in systemically infected leaves (Fig. 6a). Interestingly, TRV-BIR1 RNA accumulated in upper non-infiltrated leaves to the same levels as the TRV-GFP control, suggesting that overexpression of *BIR1* had negligible effects on TRV accumulation in *N. benthamiana* cells (Fig. 6a and S6c).

Inoculation of three-week-old *Arabidopsis* plants with TRV-BIR1 revealed the appearance of a range of morphological defects at approximately 14 dpi, affecting more than 80% of the inoculated plants (Fig. 6b). Symptoms were more severe at later stages post-infection and included stunted morphology, abnormal leaf shape, extensive leaf necrosis, loss of apical dominance during bolting (bushy phenotype) and premature death (Fig. 6b). In contrast, plants infected with TRV-GFP, used as control, developed normally like non-inoculated or mock-inoculated plants (Fig. 6b). Interestingly, morphological phenotypes of TRV-BIR1-infected individual plants coincided with extremely high levels of *BIR1* transcripts (Fig. 6c). Conversely, TRV-BIR1-infected plants that developed free of symptoms accumulated less *BIR1* transcripts, similar to the TRV-GFP-infected control plants (Fig. 6c).

Growth arrest and cell death are reminiscent of plants that show constitutive activation of defense responses (Lorrain *et al.*, 2003). To gain insight into the effects of *BIR1* overexpression in TRV-infected tissues, we measured relative transcript levels of defense genes *PR1* and *PR4*. Despite *BIR1* being a repressor of plant immunity, the expression of *PR1* and *PR4* was markedly up regulated in infected plants producing high amounts of *BIR1* transcripts (Fig. 6d). In contrast, *PR1* and *PR4* accumulated to normal levels in symptomless plants producing low amounts of *BIR1* transcripts (Fig. 6d). *PR1* and *PR4* were poorly induced in plants infected with TRV-GFP, confirming that defense activation was linked to *BIR1* overexpression rather than virus infection (Fig. 6d). These experiments suggested that *BIR1* overexpression induces constitutive immunity in *Arabidopsis*. Interestingly, TRV levels in TRV-BIR1-infected plants exhibited a marked variability between individuals and experimental replicates (Fig. 6e), and no correlation between *BIR1* transcript levels and viral accumulation was found (Bilateral Spearman correlation, $\rho = 0,48$, $p = 0,84$). We concluded that *BIR1* overdosage had no direct effects on viral susceptibility in *Arabidopsis*.

Inducible *BIR1* overexpression in transgenic *Arabidopsis* causes phenotypical defects and triggers the activation of plant defense

It is possible that the morphological phenotypes associated to high *BIR1* doses in TRV-BIR1-infected cells were due to the combined effect of *BIR1* overexpression and viral infection. To further investigate this possibility, we employed a dexamethasone (DEX)-inducible system to generate independent *Arabidopsis* homozygous lines that overexpress mCherry-tagged *BIR1* proteins (Fig. S7a,b,c,d). DEX treatment had no apparent effects on wild type Col-0

seedlings, and *BIR1* transgenics treated with water exhibited normal phenotypes (Fig. 7a and S8a,b). Conversely, more than 80% of DEX-treated *BIR1* transgenics displayed stunting, abnormal leaf shape, leaf necrosis, bushy phenotype and cell death that resembled the morphological phenotypes observed in plants infected with TRV-BIR1 (Fig. 7a and S8a,b). As predicted, DEX-treated plants showing strong phenotypes accumulated over two orders of magnitude more *BIR1* transcripts than control plants (Fig. 7b). Water-treated transgenic lines, wild type (non-transgenic) plants treated with DEX, and DEX-treated transgenics that exhibited normal growing phenotypes produced equivalent low amounts of *BIR1* transcripts (Fig. 7b). Similarly, BIR1-mCherry fusion proteins were detected at much higher intensities in plants with morphological defects than in the above controls (Fig. 7c).

When the accumulation of defense gene markers was tested, high amounts of *PR1*, *PR4*, *PAD3* or *WRKY29* transcripts accumulated in plants overexpressing *BIR1* as opposed to wild type or non-expressing transgenic plants (Fig. 7d and S8c). As predicted, none of the above markers were up regulated in asymptomatic *BIR1* transgenics (Fig. 7d and S8c). We further demonstrated that overexpression of *BIR1* triggered localized cell death in DEX-treated transgenic leaves, as deduced by trypan blue staining (Fig. 7e). These observations indicated that DEX-induced overexpression of *BIR1* stimulated an autoimmune response in an infection-free cell environment.

Discussion

BIR1 is a negative regulator of several resistance pathways in which BAK1 and SOBIR1 have concerted roles (Gao *et al.*, 2009; Dominguez-Ferrerias *et al.*, 2015; Liu *et al.*, 2016). Here we provide compelling evidence that *BIR1* transcription is positively regulated by SA and propose that TRV triggers NPR1-dependent expression of *BIR1* during the infection by increasing SA levels in the infected tissue. We show that loss of BIR1 function in the *bir1-1* mutant severely compromises TRV accumulation, likely due to constitutive activation of plant defenses in this mutant. A previous study reported that the *bir1-1* mutation leads to extensive cell death, elevated levels of SA and SA-dependent gene expression (Gao *et al.*, 2009). Based on this observation, it is possible that the SA defense pathway could prime an immune response against TRV in *bir1-1* mutants. In some compatible plant-virus interactions, SA treatment or overexpression of SA biosynthetic genes can potentiate antiviral responses by affecting virus replication, coat protein accumulation and systemic virus movement (Chivasa *et al.*, 1997; Mayers *et al.*, 2005; Ishihara *et al.*, 2008; Qi *et al.*, 2018).

However, we found that exogenous application of SA activated the SA defense pathway but was unable to antagonize the virus. Furthermore, a phenotype of strong resistance against TRV was also observed in the double *bir1-1 sobir1-1* mutant, in which cell death and constitutive expression of SA-dependent defense genes are strongly reduced by the *sobir1-1* mutation (Gao *et al.*, 2009). These findings prove that enhanced TRV resistance in *bir1-1* plants was not due to constitutive SA defense priming (Gao *et al.*, 2009). On the contrary, we observed that loss of ICS1 function in the *sid2-2* mutants correlated with reduced TRV proliferation, suggesting that SA may be important to support TRV infection. Importantly, altered susceptibility was not observed in plants expressing high levels of BIR1, even though cell death and SA-mediated defense signaling pathway were substantially enhanced in BIR1 overexpressor plants. These results suggest that defense responses that were concomitant to both low and high expression of *BIR1* may have a minor role in controlling viral proliferation in Arabidopsis. BAK1 is also required for activation of cell death and defense responses in the *bir1-1* mutant (Liu *et al.*, 2016). We show that *BAK1* transcripts were diminished in infected plants, and *bak1-5* mutants, which are impaired in PTI but not in BR signaling (Chinchilla *et al.*, 2007; Heese *et al.*, 2007; Schwessinger *et al.*, 2011), were more susceptible to infection with TRV and other viruses (Korner *et al.*, 2013). These findings suggest that BAK1, and likely SOBIR1, contribute to modulate viral proliferation, but their relationships with BIR1 and their potential interdependence during the antiviral response remain to be investigated. Furthermore, the role of NDR1-, PAD4- and EDS1-resistance pathways that are triggered in the *bir1-1* mutant needs to be investigated to elucidate their contribution to antiviral resistance (Gao *et al.*, 2009).

In our study, we prove that both transcriptional and post-transcriptional RNA silencing contribute, at least partly, to *BIR1* homeostasis. We found that RdDM constitutively regulates *BIR1*. Under non-challenging conditions, our results suggest that post-transcriptional silencing may be mobilized to perform conditional fine-tune regulation of *BIR1* expression. However, during viral infection, post-transcriptional silencing strongly reinforces the action of epigenetic silencing by removing the excess of *BIR1* transcripts produced upon *BIR1* transcriptional activation. This idea also emerges from our analysis of degradome according to which *BIR1* gives rise to high amounts of discrete cleaved 3' mRNA products in infected plants compared to mock-inoculated plants. The genetic requirement for RNA silencing components in the control of *BIR1* is consistent with the widespread accumulation of *BIR1*-derived siRNAs of sense and antisense polarities in infected plants, but not in mock-

inoculated ones. *BIR1* siRNAs resemble viral-associated siRNAs (vasiRNAs) that are produced from multiple host genes during activation of antiviral silencing (Cao *et al.*, 2014). vasiRNAs are competent in directing silencing of the host target genes in line with the idea that *BIR1* siRNAs guide autosilencing of *BIR1* transcripts. The requirement for *BIR1* siRNA biogenesis and function seems to differ however from the predicted genetic pathway of vasiRNAs, which are mostly dependent on DCL4, RDR1 and AGO2 (Cao *et al.*, 2014). From our data, it is possible that several complementary pathways that include RDR6 and AGO1 also contribute to vasiRNA biogenesis and function during viral infections.

We found that the strong overexpression of *BIR1* triggers autoimmune phenotypes similar to those observed in *bir1-1* mutants (Gao *et al.*, 2009), indicating that a well-calibrated regulation of *BIR1* guarantees a proper control of immune signaling pathways. Given that BIR1 is an active RLKs, overexpression of BIR1 may interfere with other closely related RLKs causing miscoordination of cellular signaling pathways, including plant defense or development. For instance, high levels of BIR1 may hinder BAK1-mediated regulation of SOBIR1-independent cell death (Liu *et al.*, 2016). Although BIR1 represses immune responses in normal growing conditions, we demonstrated that BIR1 triggers plant defenses when expressed at a high dose, even in the absence of virus. As a plausible explanation, overproduction of BIR1 may either affect BIR1-dependent negative regulation of (co)receptor partners or, alternatively, promote inappropriate interactions with other immune (co)receptor proteins that result in the activation of resistance (Prelich, 2012; Rodriguez *et al.*, 2016).

We saw that Arabidopsis mutants with defects in RdDM or siRNA biogenesis/function produce BIR1 at levels that barely compromise normal plant development. This finding has two important implications. First, one could argue that RNA silencing plays a secondary role in controlling BIR1 expression and that other yet unknown mechanisms provide additional layers of regulation that ultimately confine BIR1 below detrimental levels for plant fitness. This is a reasonable possibility, however, loss of function of one or several silencing genes does not necessarily imply a complete inhibition of the pathway (Bouche *et al.*, 2006). And importantly, mutants tested in this study were affected either in the RdDM pathway or in the post-transcriptional silencing pathway, but not both. As a result, it is likely that residual RNA silencing activities in these mutants could yet exert effective *BIR1* control preventing BIR1 from reaching deleterious expression levels upon virus or pathogen (SA-mediated) induction. The second implication is that phenotypes associated to *BIR1* induction are likely dose-dependent. In our experiments, plants infected with TRV-BIR1 or DEX-treated transgenic

plants showing developmental defects produced more than two orders of magnitude *BIR1* transcripts than control plants. Conversely, we observed that seedlings of the same transgenic lines developed normally when they were grown on MS-DEX plates (Fig. S9a). In these experimental conditions transgenic plants accumulated only ten to 20 times more *BIR1* transcripts than the wild type plants (Fig. S9b). This represented at least an order of magnitude less expression than that observed in DEX-treated, soil-grown plants. Furthermore, accumulation of defense genes was not substantially altered in transgenic seedlings (lines 5 and 6) grown on plates (Fig. S9c). Only, transgenic line 9 produced *BIR1* transcripts at levels that triggered a modest induction of *PR1*, *PR4* and *PAD3*, but they were insufficient to perturb normal development (Fig. S9c). A dose-dependent mechanism would explain why silencing mutants, in which increments in *BIR1* expression were only mild, display normal phenotypes. Interestingly, *ddc* mutants show a suite of developmental abnormalities (Chan *et al.*, 2006) and activation of defense genes (Fig. S9d) (Downen *et al.*, 2012), but morphological phenotypes in these plants are likely due to a broad misregulation of developmental genes that are normally controlled by non-CG methylation (Chan *et al.*, 2006). *BIR1* belongs to the *BIR* family, with four members of which *BIR2* and *BIR3* also function as negative regulators of BAK1-mediated immunity (Halter *et al.*, 2014; Imkampe *et al.*, 2017). Transgenic overexpression of *BIR3* in Arabidopsis also leads to dwarf phenotypes that were dosage-dependent (Imkampe *et al.*, 2017). From our experiments we conclude that regulation of *BIR1* is critical for plant viability, and propose that the proper *BIR1* functioning requires a threshold expression, and once *BIR1* exceeds or falls behind such a threshold, misregulation of plant immunity takes place. Interestingly, in a previous study *BIR1* transgenic Arabidopsis under a 35S promoter exhibited wild type morphology, and PTI responses were not apparently affected in these plants, suggesting that the *BIR1* transgene was expressed at non-detrimental levels in their experimental conditions (Liu *et al.*, 2016).

In conclusion, our results demonstrate that plant viruses initiate a basal immune response that involves SA-dependent activation of the immune repressor *BIR1*. We propose that *BIR1* acts as a negative regulator of antiviral defense in Arabidopsis. Regulation of *BIR1* gene expression is important to avoid constitutive defense responses that negatively impact plant development and fitness. In this scenario, RNA silencing provides two complementary layers of transcriptional and post-transcriptional regulation that prevent, alone or in conjunction with other regulatory mechanisms, *BIR1* from reaching deleterious expression levels when *BIR1* is

transcriptionally activated (Fig. S10a,b). Our work provides novel mechanistic insights into the regulation of BIR1 homeostasis that may be common for other plant immune components.

Acknowledgements

This work has been supported by FPI fellowships (BES-2013-063138 and EEBB-I-16-10815) to IG-B, by a Ramon y Cajal grant (RyC-2011-07006) to VR-F and by National Research grants (BIO2012-39973 and BIO2015-70752-R) to CL from Ministerio de Economía y Competitividad (MINECO/FEDER), Spain, and by a National Institutes of Health (USA) grant R01GM108722 to ATW. We thank Yuelin Zhang, James Carrington, Steve Jacobsen, Craig Pikaard, Xinniang Dong and Eric Richards for providing seeds, and Ignacio Hamada, Jan Kuciński, Shriya Sethuraman and M. Hafiz Rothi for technical assistance.

Author contributions

CL conceived and designed the study; IG-B, LD, ATW and CL outlined experiments; IG-B, LD, VA-S, JGV, AE, VR-F and CL performed research; LD and CL contributed with informatic analysis; IG-B, LD, ATW and CL analyzed data; and CL wrote the paper.

REFERENCES

- Addo-Quaye C, Miller W, Axtell MJ. 2009.** CleaveLand: a pipeline for using degradome data to find cleaved small RNA targets. *Bioinformatics* **25**(1): 130-131.
- Boccaro M, Sarazin A, Thiebauld O, Jay F, Voinnet O, Navarro L, Colot V. 2014.** The *Arabidopsis* miR472-RDR6 silencing pathway modulates PAMP- and effector-triggered immunity through the post-transcriptional control of disease resistance genes. *PLoS Pathog* **10**(1): e1003883.
- Bohmdorfer G, Rowley MJ, Kucinski J, Zhu Y, Amies I, Wierzbicki AT. 2014.** RNA-directed DNA methylation requires stepwise binding of silencing factors to long non-coding RNA. *Plant J* **79**(2): 181-191.
- Bohmdorfer G, Sethuraman S, Rowley MJ, Krzyszton M, Rothi MH, Bouzit L, Wierzbicki AT. 2016.** Long non-coding RNA produced by RNA polymerase V determines boundaries of heterochromatin. *eLife* **5**: e19092.

- Boller T, Felix G. 2009.** A renaissance of elicitors: perception of microbe-associated molecular patterns and danger signals by pattern-recognition receptors. *Annu Rev Plant Biol* **60**: 379-406.
- Bouche N, Lauressergues D, Gascioli V, Vaucheret H. 2006.** An antagonistic function for *Arabidopsis* DCL2 in development and a new function for DCL4 in generating viral siRNAs. *EMBO J* **25**(14): 3347-3356.
- Campo S, Peris-Peris C, Sire C, Moreno AB, Donaire L, Zytnicki M, Notredame C, Llave C, San Segundo B. 2013.** Identification of a novel microRNA (miRNA) from rice that targets an alternatively spliced transcript of the *Nramp6* (*Natural resistance-associated macrophage protein 6*) gene involved in pathogen resistance. *New Phytol* **199**(1): 212-227.
- Cao H, Glazebrook J, Clarke JD, Volko S, Dong X. 1997.** The *Arabidopsis* *NPR1* gene that controls systemic acquired resistance encodes a novel protein containing ankyrin repeats. *Cell* **88**(1): 57-63.
- Cao M, Du P, Wang X, Yu YQ, Qiu YH, Li W, Gal-On A, Zhou C, Li Y, Ding SW. 2014.** Virus infection triggers widespread silencing of host genes by a distinct class of endogenous siRNAs in *Arabidopsis*. *Proc Natl Acad Sci U S A* **111**(40): 14613-14618.
- Cao X, Jacobsen SE. 2002.** Locus-specific control of asymmetric and CpNpG methylation by the *DRM* and *CMT3* methyltransferase genes. *Proc Natl Acad Sci U S A* **99** Suppl 4: 16491-16498.
- Chan SW, Henderson IR, Zhang X, Shah G, Chien JS, Jacobsen SE. 2006.** RNAi, DRD1, and histone methylation actively target developmentally important non-CG DNA methylation in *Arabidopsis*. *PLoS Genet* **2**(6): e83.
- Chen Z, Zheng Z, Huang J, Lai Z, Fan B. 2009.** Biosynthesis of salicylic acid in plants. *Plant Signal Behav* **4**(6): 493-496.
- Chinchilla D, Zipfel C, Robatzek S, Kemmerling B, Nurnberger T, Jones JD, Felix G, Boller T. 2007.** A flagellin-induced complex of the receptor FLS2 and BAK1 initiates plant defence. *Nature* **448**(7152): 497-500.
- Chivasa S, Murphy AM, Naylor M, Carr JP. 1997.** Salicylic acid interferes with *Tobacco Mosaic Virus* replication via a novel salicylhydroxamic acid-sensitive mechanism. *Plant Cell* **9**(4): 547-557.
- Clough SJ, Bent AF. 1998.** Floral dip: a simplified method for *Agrobacterium*-mediated transformation of *Arabidopsis thaliana*. *Plant J* **16**(6): 735-743.

- Coll NS, Epple P, Dangl JL. 2011.** Programmed cell death in the plant immune system. *Cell Death Differ* **18**(8): 1247-1256.
- Dangl JL, Jones JD. 2001.** Plant pathogens and integrated defence responses to infection. *Nature* **411**(6839): 826-833.
- Diaz-Tielas C, Grana E, Sotelo T, Reigosa MJ, Sanchez-Moreiras AM. 2012.** The natural compound trans-chalcone induces programmed cell death in *Arabidopsis thaliana* roots. *Plant Cell Environ* **35**(8): 1500-1517.
- Dodds PN, Rathjen JP. 2010.** Plant immunity: towards an integrated view of plant-pathogen interactions. *Nat Rev Genet* **11**(8): 539-548.
- Dominguez-Ferreras A, Kiss-Papp M, Jehle AK, Felix G, Chinchilla D. 2015.** An overdose of the *Arabidopsis* coreceptor BRASSINOSTEROID INSENSITIVE1-ASSOCIATED RECEPTOR KINASE1 or its ectodomain causes autoimmunity in a SUPPRESSOR OF BIR1-1-dependent manner. *Plant Physiol* **168**(3): 1106-1121.
- Donaire L, Pedrola L, de la Rosa R, Llave C. 2011.** High-throughput sequencing of RNA silencing-associated small RNAs in olive (*Olea europaea* L.). *PLoS ONE* **6**(11): e27916.
- Dowen RH, Pelizzola M, Schmitz RJ, Lister R, Dowen JM, Nery JR, Dixon JE, Ecker JR. 2012.** Widespread dynamic DNA methylation in response to biotic stress. *Proc Natl Acad Sci U S A* **109**(32): E2183-2191.
- Fernandez-Calvino L, Guzman-Benito I, Del Toro FJ, Donaire L, Castro-Sanz AB, Ruiz-Ferrer V, Llave C. 2016a.** Activation of senescence-associated *Dark-inducible (DIN)* genes during infection contributes to enhanced susceptibility to plant viruses. *Mol Plant Pathol* **17**(1): 3-15.
- Fernandez-Calvino L, Martinez-Priego L, Szabo EZ, Guzman-Benito I, Gonzalez I, Canto T, Lakatos L, Llave C. 2016b.** Tobacco rattle virus 16K silencing suppressor binds ARGONAUTE 4 and inhibits formation of RNA silencing complexes. *J Gen Virol* **97**(1): 246-257.
- Fernandez-Calvino L, Osorio S, Hernandez ML, Hamada IB, Del Toro FJ, Donaire L, Yu A, Bustos R, Fernie AR, Martinez-Rivas JM, et al. 2014.** Virus-induced alterations in primary metabolism modulate susceptibility to *Tobacco rattle virus* in *Arabidopsis*. *Plant Physiol* **166**(4): 1821-1838.
- Gao M, Wang X, Wang D, Xu F, Ding X, Zhang Z, Bi D, Cheng YT, Chen S, Li X, et al. 2009.** Regulation of cell death and innate immunity by two receptor-like kinases in *Arabidopsis*. *Cell Host Microbe* **6**(1): 34-44.

- German MA, Luo S, Schroth G, Meyers BC, Green PJ. 2009.** Construction of Parallel Analysis of RNA Ends (PARE) libraries for the study of cleaved miRNA targets and the RNA degradome. *Nat Protoc* **4**(3): 356-362.
- German MA, Pillay M, Jeong DH, Hetawal A, Luo S, Janardhanan P, Kannan V, Rymarquis LA, Nobuta K, German R, et al. 2008.** Global identification of microRNA-target RNA pairs by parallel analysis of RNA ends. *Nat Biotechnol* **26**(8): 941-946.
- Gouveia BC, Calil IP, Machado JP, Santos AA, Fontes EP. 2016.** Immune receptors and co-receptors in antiviral innate immunity in plants. *Front Microbiol* **7**: 2139.
- Halter T, Imkampe J, Mazzotta S, Wierzba M, Postel S, Bucherl C, Kiefer C, Stahl M, Chinchilla D, Wang X, et al. 2014.** The leucine-rich repeat receptor kinase BIR2 is a negative regulator of BAK1 in plant immunity. *Curr Biol* **24**(2): 134-143.
- He XF, Fang YY, Feng L, Guo HS. 2008.** Characterization of conserved and novel microRNAs and their targets, including a TuMV-induced TIR-NBS-LRR class R gene-derived novel miRNA in *Brassica*. *FEBS Lett* **582**(16): 2445-2452.
- He XJ, Hsu YF, Pontes O, Zhu J, Lu J, Bressan RA, Pikaard C, Wang CS, Zhu JK. 2009.** NRPD4, a protein related to the RPB4 subunit of RNA polymerase II, is a component of RNA polymerases IV and V and is required for RNA-directed DNA methylation. *Genes Dev* **23**(3): 318-330.
- Heese A, Hann DR, Gimenez-Ibanez S, Jones AM, He K, Li J, Schroeder JI, Peck SC, Rathjen JP. 2007.** The receptor-like kinase SERK3/BAK1 is a central regulator of innate immunity in plants. *Proc Natl Acad Sci U S A* **104**(29): 12217-12222.
- Imkampe J, Halter T, Huang S, Schulze S, Mazzotta S, Schmidt N, Manstretta R, Postel S, Wierzba M, Yang Y, et al. 2017.** The *Arabidopsis* leucine-rich repeat receptor kinase BIR3 negatively regulates BAK1 receptor complex formation and stabilizes BAK1. *Plant Cell* **29**(9): 2285-2303.
- Ishihara T, Sekine KT, Hase S, Kanayama Y, Seo S, Ohashi Y, Kusano T, Shibata D, Shah J, Takahashi H. 2008.** Overexpression of the *Arabidopsis thaliana* *EDS5* gene enhances resistance to viruses. *Plant Biol (Stuttg)* **10**(4): 451-461.
- Johansen LK, Carrington JC. 2001.** Silencing on the spot. Induction and suppression of RNA silencing in the *Agrobacterium*-mediated transient expression system. *Plant Physiol* **126**(3): 930-938.
- Jones JD, Dangl JL. 2006.** The plant immune system. *Nature* **444**(7117): 323-329.
- Katiyar-Agarwal S, Gao S, Vivian-Smith A, Jin H. 2007.** A novel class of bacteria-induced small RNAs in *Arabidopsis*. *Genes Dev* **21**(23): 3123-3134.

- Katiyar-Agarwal S, Morgan R, Dahlbeck D, Borsani O, Villegas A, Jr., Zhu JK, Staskawicz BJ, Jin H. 2006.** A pathogen-inducible endogenous siRNA in plant immunity. *Proc Natl Acad Sci U S A* **103**(47): 18002-18007.
- Korner CJ, Klauser D, Niehl A, Dominguez-Ferreras A, Chinchilla D, Boller T, Heinlein M, Hann DR. 2013.** The immunity regulator BAK1 contributes to resistance against diverse RNA viruses. *Mol Plant Microbe Interact* **26**(11): 1271-1280.
- Lellis AD, Kasschau KD, Whitham SA, Carrington JC. 2002.** Loss-of-susceptibility mutants of *Arabidopsis thaliana* reveal an essential role for eIF(iso)4E during potyvirus infection. *Curr Biol* **12**(12): 1046-1051.
- Li F, Pignatta D, Bendix C, Brunkard JO, Cohn MM, Tung J, Sun H, Kumar P, Baker B. 2012.** MicroRNA regulation of plant innate immune receptors. *Proc Natl Acad Sci U S A* **109**(5): 1790-1795.
- Li Y, Lu YG, Shi Y, Wu L, Xu YJ, Huang F, Guo XY, Zhang Y, Fan J, Zhao JQ, et al. 2014.** Multiple rice microRNAs are involved in immunity against the blast fungus *Magnaporthe oryzae*. *Plant Physiol* **164**(2): 1077-1092.
- Li Y, Zhang Q, Zhang J, Wu L, Qi Y, Zhou JM. 2010.** Identification of microRNAs involved in pathogen-associated molecular pattern-triggered plant innate immunity. *Plant Physiol* **152**(4): 2222-2231.
- Liu Y, Huang X, Li M, He P, Zhang Y. 2016.** Loss-of-function of *Arabidopsis* receptor-like kinase BIR1 activates cell death and defense responses mediated by BAK1 and SOBIR1. *New Phytol* **212**(3): 637-645.
- Liu Y, Schiff M, Marathe R, Dinesh-Kumar SP. 2002.** Tobacco *Rar1*, *EDS1* and *NPRI/NIMI* like genes are required for N-mediated resistance to *Tobacco mosaic virus*. *Plant J* **30**(4): 415-429.
- Lopez Sanchez A, Stassen JH, Furci L, Smith LM, Ton J. 2016.** The role of DNA (de)methylation in immune responsiveness of *Arabidopsis*. *Plant J* **88**(3): 361-374.
- Lorrain S, Vaillau F, Balague C, Roby D. 2003.** Lesion mimic mutants: keys for deciphering cell death and defense pathways in plants? *Trends Plant Sci* **8**(6): 263-271.
- Ma C, Liu Y, Bai B, Han Z, Tang J, Zhang H, Yaghmaiean H, Zhang Y, Chai J. 2017.** Structural basis for BIR1-mediated negative regulation of plant immunity. *Cell Res* **27**(12): 1521-1524.
- Marques-Bueno MDM, Morao AK, Cayrel A, Platre MP, Barberon M, Caillieux E, Colot V, Jaillais Y, Roudier F, Vert G. 2016.** A versatile Multisite Gateway-compatible

- promoter and transgenic line collection for cell type-specific functional genomics in *Arabidopsis*. *Plant J* **85**(2): 320-333.
- Martin GB, Bogdanove AJ, Sessa G. 2003.** Understanding the functions of plant disease resistance proteins. *Annu Rev Plant Biol* **54**: 23-61.
- Mayers CN, Lee KC, Moore CA, Wong SM, Carr JP. 2005.** Salicylic acid-induced resistance to *Cucumber mosaic virus* in squash and *Arabidopsis thaliana*: contrasting mechanisms of induction and antiviral action. *Mol Plant Microbe Interact* **18**(5): 428-434.
- Meyers BC, Kozik A, Griego A, Kuang H, Michelmore RW. 2003.** Genome-wide analysis of NBS-LRR-encoding genes in *Arabidopsis*. *Plant Cell* **15**(4): 809-834.
- Navarro L, Dunoyer P, Jay F, Arnold B, Dharmasiri N, Estelle M, Voinnet O, Jones JD. 2006.** A plant miRNA contributes to antibacterial resistance by repressing auxin signaling. *Science* **312**(5772): 436-439.
- Navarro L, Jay F, Nomura K, He SY, Voinnet O. 2008.** Suppression of the microRNA pathway by bacterial effector proteins. *Science* **321**(5891): 964-967.
- Nicaise V, Candresse T. 2017.** Plum pox virus capsid protein suppresses plant pathogen-associated molecular pattern (PAMP)-triggered immunity. *Mol Plant Pathol* **18**(6): 878-886.
- Ouyang S, Park G, Atamian HS, Han CS, Stajich JE, Kaloshian I, Borkovich KA. 2014.** MicroRNAs suppress NB domain genes in tomato that confer resistance to *Fusarium oxysporum*. *PLoS Pathog* **10**(10): e1004464.
- Patterson K, Molloy L, Qu W, Clark S. 2011.** DNA methylation: bisulphite modification and analysis. *J Vis Exp* **56**: 3170.
- Prelich G. 2012.** Gene overexpression: uses, mechanisms, and interpretation. *Genetics* **190**(3): 841-854.
- Qi G, Chen J, Chang M, Chen H, Hall K, Korin J, Liu F, Wang D, Fu ZQ. 2018.** Pandemonium breaks out: Disruption of salicylic acid-mediated defense by plant pathogens. *Mol Plant* **11**(12): 1427-1439.
- Rodriguez E, El Ghouh H, Mundy J, Petersen M. 2016.** Making sense of plant autoimmunity and 'negative regulators'. *FEBS J* **283**(8): 1385-1391.
- Rowley MJ, Avrutsky MI, Sifuentes CJ, Pereira L, Wierzbicki AT. 2011.** Independent chromatin binding of ARGONAUTE4 and SPT5L/KTF1 mediates transcriptional gene silencing. *PLoS Genet* **7**(6): e1002120.

- Schwessinger B, Roux M, Kadota Y, Ntoukakis V, Sklenar J, Jones A, Zipfel C. 2011.** Phosphorylation-dependent differential regulation of plant growth, cell death, and innate immunity by the regulatory receptor-like kinase BAK1. *PLoS Genet* **7**(4): e1002046.
- Shivaprasad PV, Chen HM, Patel K, Bond DM, Santos BA, Baulcombe DC. 2012.** A microRNA superfamily regulates nucleotide binding site-leucine-rich repeats and other mRNAs. *Plant Cell* **24**(3): 859-874.
- Stroud H, Greenberg MV, Feng S, Bernatavichute YV, Jacobsen SE. 2013.** Comprehensive analysis of silencing mutants reveals complex regulation of the *Arabidopsis* methylome. *Cell* **152**(1-2): 352-364.
- Takahashi Y, Nasir KH, Ito A, Kanzaki H, Matsumura H, Saitoh H, Fujisawa S, Kamoun S, Terauchi R. 2007.** A high-throughput screen of cell-death-inducing factors in *Nicotiana benthamiana* identifies a novel MAPKK that mediates INF1-induced cell death signaling and non-host resistance to *Pseudomonas cichorii*. *Plant J* **49**(6): 1030-1040.
- Tena G, Boudsocq M, Sheen J. 2011.** Protein kinase signaling networks in plant innate immunity. *Curr Opin Plant Biol* **14**(5): 519-529.
- Vallarino JG, Osorio S. 2016.** Simultaneous determination of plant hormones by GC-TOF-MS. *Methods Mol Biol* **1363**: 229-237.
- Wierzbicki AT, Cocklin R, Mayampurath A, Lister R, Rowley MJ, Gregory BD, Ecker JR, Tang H, Pikaard CS. 2012.** Spatial and functional relationships among Pol V-associated loci, Pol IV-dependent siRNAs, and cytosine methylation in the *Arabidopsis* epigenome. *Genes Dev* **26**(16): 1825-1836.
- Wildermuth MC, Dewdney J, Wu G, Ausubel FM. 2001.** Isochorismate synthase is required to synthesize salicylic acid for plant defence. *Nature* **414**(6863): 562-565.
- Wu Y, Zhang D, Chu JY, Boyle P, Wang Y, Brindle ID, De Luca V, Despres C. 2012.** The *Arabidopsis* NPR1 protein is a receptor for the plant defense hormone salicylic acid. *Cell Rep* **1**(6): 639-647.
- Xiao YL, Redman JC, Monaghan EL, Zhuang J, Underwood BA, Moskal WA, Wang W, Wu HC, Town CD. 2010.** High throughput generation of promoter reporter (GFP) transgenic lines of low expressing genes in *Arabidopsis* and analysis of their expression patterns. *Plant Methods* **6**: 18.
- Xie M, Yu B. 2015.** siRNA-directed DNA methylation in plants. *Curr Genomics* **16**(1): 23-31.

- Yi H, Richards EJ. 2007.** A cluster of disease resistance genes in *Arabidopsis* is coordinately regulated by transcriptional activation and RNA silencing. *Plant Cell* **19**(9): 2929-2939.
- Yu A, Lepere G, Jay F, Wang J, Bapaume L, Wang Y, Abraham AL, Penterman J, Fischer RL, Voinnet O, et al. 2013.** Dynamics and biological relevance of DNA demethylation in *Arabidopsis* antibacterial defense. *Proc Natl Acad Sci U S A* **110**(6): 2389-2394.
- Zhai J, Jeong DH, De Paoli E, Park S, Rosen BD, Li Y, Gonzalez AJ, Yan Z, Kitto SL, Grusak MA, et al. 2011.** MicroRNAs as master regulators of the plant NB-LRR defense gene family via the production of phased, trans-acting siRNAs. *Genes Dev* **25**(23): 2540-2553.
- Zhang X, Zhao H, Gao S, Wang WC, Katiyar-Agarwal S, Huang HD, Raikhel N, Jin H. 2011.** *Arabidopsis* Argonaute 2 regulates innate immunity via miRNA393(*)-mediated silencing of a Golgi-localized SNARE gene, *MEMB12*. *Mol Cell* **42**(3): 356-366.
- Zvereva AS, Pooggin MM. 2012.** Silencing and innate immunity in plant defense against viral and non-viral pathogens. *Viruses* **4**(11): 2578-2597.

SUPPORTING INFORMATION

Figure S1. Effect of RNA silencing on *BIR1* expression in plants infected with TuMV.

Figure S2. Epigenetic regulation of *BIR1* and RdDM-methylation controls.

Figure S3. Methylation status of the *BIR1* promoter using whole-genome bisulfite sequencing (WGBS) data in *Arabidopsis*.

Figure S4. Methylation status of the *BIR1* promoter using in-house bisulfite sequencing in *Arabidopsis*.

Figure S5. Epigenetic regulation of *BIR1* and RdDM-methylation controls in salicylic acid (SA)-treated plants.

Figure S6. *BIR1* mRNA accumulation in RNA silencing mutants, cleavage mapping at the 5' UTR of *BIR1* mRNA and viral accumulation in *N. benthamiana* leaves expressing *BIR1*.

Figure S7. DEX-inducible system for overexpression of *BIR1* in *Arabidopsis* plants.

Figure S8. Phenotypes of *BIR1* overexpressing transgenic *Arabidopsis*.

Figure S9. Phenotypes of *BIR1* overexpressing transgenic seedlings grown in axenic conditions.

Figure S10. Model of *BIR1* regulation

Table S1. List of primers.

FIGURE LEGENDS

Figure 1. Expression of *BIR1*, *SOBIR1* and *BAK1* during TRV infection in Arabidopsis and effect of their loss-of-function mutations on TRV accumulation. **(a)** Time-course accumulation of *BIR1* transcripts in mock-inoculated and TRV-infected leaves. **(b)** Accumulation of TRV genomic RNA in TRV-infected rosette leaves of Arabidopsis wild type (Col-0), *bir1-1* mutants (lelf) and two *bir1-1/BIR1-HA* complemented lines (L17 and L49) (right) at 8 days post-inoculation (dpi). Mock-inoculated controls were included in the left panel to discriminate background amplification. The phenotype of wild type and *bir1-1* plants grown on MS medium at 21° C is shown. **(c)** Western blot analysis of BIR1 proteins in extracts from leaves of mock-inoculated (-) or TRV-infected (+) *bir1-1/BIR1-HA* complemented lines (L17 and L49) at 8 dpi. Ponceau staining was used as a protein loading control. **(d)** Accumulation of defense-related *PR1*, *PR4*, and *WRKY29* transcripts in mock-inoculated or TRV-infected leaves of Arabidopsis wild type and *bir1-1* mutants at 8 dpi. **(e)** Time-course accumulation of *SOBIR1* transcripts in mock-inoculated and TRV-infected leaves. **(f)** Time-course accumulation of *BAK1* transcripts in TRV-infected and mock-inoculated leaves. **(g)** Accumulation of TRV genomic RNA in rosette leaves of wild type and *bak1-5* mutants at 8 dpi. **(h)** Accumulation of TRV genomic RNA in rosette leaves of wild type, *sobir1-12* and *sobir1 bir1* mutants at 8 dpi. **(i)** Accumulation of *PR1* transcripts (left) and TRV genomic RNA (right) in rosette leaves of wild type plants treated with or without (mock) salicylic acid (SA). Exp #1 and #2 are described in Materials and methods. Relative expression levels were determined by qRT-PCR and normalized to the *CBP20* internal control. Error bars represent SD from three independent PCR measurements. Values in (a), (e) and (f) are related to the mock-inoculated sample at 3 dpi that was arbitrarily assigned to 1. Asterisks (Student's *t* test) or different letters (one-way ANOVA) were used to indicate significant differences ($P < 0.001$). The experiments were repeated at least three times with similar results and one representative biological replicate is shown.

Figure 2. RdDM-mediated transcriptional regulation of *BIR1*. **(a)** Distribution of *BIR1*-derived siRNAs in rosette leaves of mock-inoculated *Arabidopsis* plants (upper diagram). Sense (black dots) and antisense (red dots) siRNA species are represented as positive and negative values on the *y*-axis, respectively. The triangle graph represents the genomic distribution (percentage) of sRNAs in the sequenced set. *N* denotes the total number of filtered sequenced reads. The circle graph represents the size distribution of *BIR1*-derived siRNAs. Genome browser screenshot of CHH methylation and Pol V transcripts at the *BIR1* promoter in wild type (Col-0) and *nrpe1* mutants using WGBS and Pol V (NRPE1) RIP-seq datasets is shown (Wierzbicki *et al.*, 2012; Bohmdorfer *et al.*, 2016) (lower diagram). **(b)** Accumulation of *BIR1* transcripts in rosette leaves of wild type and RdDM mutants (*cmt3*, *drm2*, *ddc*, *nrpe1* and *ago4*). **(c)** Accumulation of Pol V-dependent *BIR1* promoter transcripts in rosette leaves of wild type and *nrpe1* mutants. **(d)** Extent of asymmetric (CHH) cytosine methylation at the *BIR1* promoter determined by chop-qPCR in rosette leaves of wild type and RdDM mutants (*nrpe1*, *drm2* and *ago4*). PCR-amplified regions contain recognition sites of the methylation-sensitive *DdeI* and *NlaIII* endonucleases. Relative expression levels were determined by qRT-PCR and normalized to the *CBP20* or *Actin2* internal control as indicated. Error bars represent SD from three independent PCR measurements. Asterisks (Student's *t* test) or different letters (one-way ANOVA) were used to indicate significant differences ($P < 0.001$). The experiments were repeated at least three times with similar results and one representative biological replicate is shown.

Figure 3. Salicylic acid (SA)-mediated transcriptional activation of *BIR1* during viral infection. **(a)** Histochemical localization of GUS expression in mock-inoculated and TRV-infected transgenic *Arabidopsis* plants expressing a GFP:GUS fusion protein under the control of the *BIR1* promoter (left panel). Northern blot analysis was used to monitor the expression of GFP:GUS mRNA using a GFP-specific radiolabeled probe (right panel). Ethidium-bromide stained RNA (prior to transfer) is shown as loading control. **(b)** Differential expression of SA biosynthetic genes *ICS1* and *PAD4*. Fold-change (\log_2) in TRV-infected plants relative to mock-inoculated ones detected using a CATMA microarray (GSE15557) (Fernandez-Calvino *et al.*, 2014). **(c)** Time-course accumulation of SA determined by GC-TOF-MS in leaves from non-inoculated, mock-inoculated and TRV-infected *Arabidopsis*. Error bars represent SD from five independent biological replicates. **(d)**

Accumulation of *BIR1* transcripts in rosette leaves of wild type (Col-0) plants treated with (+) or without (-) SA as indicated. **(e)** Northern blot analysis of GFP:GUS mRNA in extracts from transgenic leaves treated with (+) or without (-) SA as indicated. Samples were collected at 0, 6, 12 and 24 h post-treatment and blots were hybridized with a GFP-specific DNA radiolabeled probe. Ethidium-bromide stained RNA (prior to transfer) is shown as loading control. The relative accumulation (RA) level for each sample is indicated (level in mock-treated plants at 0 h was arbitrarily set at 1.0). **(f)** Accumulation of *BIR1* transcripts in mock-inoculated and TRV-infected rosette leaves of wild type and *sid2-2* mutants at 8 days post-inoculation (dpi). **(g)** Accumulation of *BIR1* transcripts in mock-inoculated and TRV-infected rosette leaves of wild type, NPR1 overexpressor and *npr1-1* mutants at 8 dpi. **(h)** Accumulation of TRV genomic RNA in rosette leaves of wild type, *npr1-1* and *sid2-2* mutants at 8 dpi. Relative expression levels were determined by qRT-PCR and normalized to the *CBP20* internal control. Unless otherwise indicated, error bars represent SD from three independent PCR measurements. Asterisks (Student's *t* test) or different letters (one-way ANOVA) were used to indicate significant differences ($P < 0.001$). The experiments were repeated at least twice with similar results and one representative biological replicate is shown.

Figure 4. *BIR1* methylation status in TRV-infected Arabidopsis. **(a)** Distribution of *BIR1*-derived siRNAs in rosette leaves of TRV-infected Arabidopsis plants. Sense (black dots) and antisense (red dots) siRNA species are represented as positive and negative values on the *y*-axis, respectively. The triangle graph represents the genomic distribution (percentage) of sRNAs in the sequenced set. N denotes the total number of filtered sequenced reads. The circle graph represents the size distribution of *BIR1*-derived siRNAs in TRV-infected plants. **(b)** Extent of asymmetric cytosine methylation at the *BIR1* promoter determined by chop-qPCR in rosette leaves of mock-inoculated and TRV-infected plants at 8 days post-inoculation (dpi). The genomic DNA was digested with methylation-sensitive enzymes *DdeI* and *NlaIII* and qPCR amplified. Non-digested (ND) plants were used as control. Values were normalized to the *Actin2* internal control. Error bars represent SD from three independent biological replicates. **(c)** Accumulation of *BIR1* transcripts in rosette leaves of mock-inoculated and TRV-infected plants of wild type (Col-0) and RdDM mutants (*cmt3*, *drm2*, *ddc*, *npr1* and *ago4*) at 8 dpi. Relative values were determined by qRT-PCR and normalized to the *CBP20* internal control. Error bars represent SD from three independent PCR

measurements. **(d)** Percentage of total cytosine methylation (left) and CG, CHG and CHH methylation (right) determined by in-house bisulfite sequencing at the *BIR1* promoter in healthy (non-inoculated), mock-inoculated and TRV-infected *Arabidopsis* at 8 dpi. H represents A, T or C. Asterisks (Student's *t* test) or different letters (one-way ANOVA) were used to indicate significant differences ($P < 0.001$). The experiments were repeated at least three times with similar results and one representative biological replicate is shown.

Figure 5. *BIR1* mRNA accumulation in RNA silencing mutants and parallel-analysis of cDNA Ends (PARE)-based identification of preferential cleavage sites within the *BIR1* mRNA. **(a)** Accumulation of *BIR1* transcripts in mock-inoculated and TRV-infected *Arabidopsis* rosette leaves of wild type (Col-0) and mutants impaired in siRNA biogenesis [*dcl2 dcl3 (dcl2/3)*, *dcl2 dcl4 (dcl2/4)*, *dcl3 dcl4 (dcl3/4)* or *dcl2 dcl3 dcl4 (dcl2/3/4)*], secondary siRNA biogenesis [*rdr1 rdr2 (rdr1/2)*, *rdr2 rdr6 (rdr2/6)*, *rdr1 rdr6 (rdr1/6)* or *rdr1 rdr2 rdr6 (rdr1/2/6)*], and AGO1 function (*ago1*). Relative expression levels were determined at 8 days post-inoculation (dpi) by qRT-PCR and normalized to the *CBP20* internal control. Error bars represent SD from three independent PCR measurements. Different letters indicate significant differences according to one-way ANOVA and Duncan test ($P < 0.001$). The experiments were repeated at least three times with similar results and one representative biological replicate is shown. **(b)** Target plots showing 5' signature abundance throughout the *BIR1* mRNA identified through degradome sequencing. Circles in the t-plots denote highly abundant signatures at the indicated positions (referred to as A, B and C) identified in TRV-infected plants but not in mock-inoculated controls. Samples from rosette leaves and inflorescences were analyzed. N denotes the total number of filtered sequenced reads.

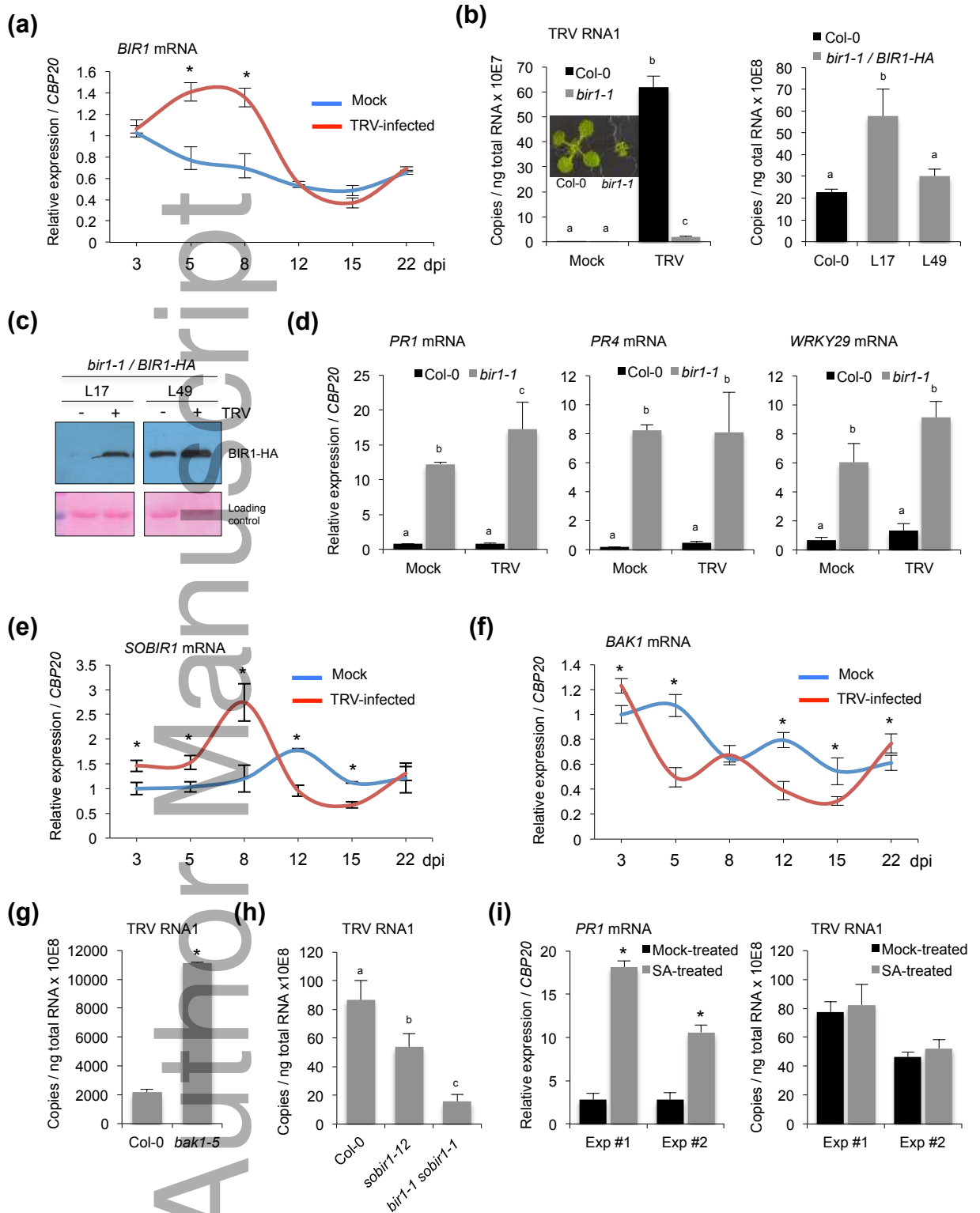
Figure 6. Phenotypes of TRV-BIR1-infected *Arabidopsis*. **(a)** TRV-derived constructs for HA-tagged expression of BIR1. The 5'UTR-containing BIR1 coding sequence was inserted adjacent to the PEBV replicase promoter in pTRV2. pTRV1 and pTRV2-BIR1 constructs were agroinjected in *N. benthamiana*. Accumulation of TRV genomic RNA in upper leaves of TRV-BIR1-infected plants at 5 days post-inoculation (dpi) is shown (left). Western blot analysis of HA-tagged BIR1 proteins in extracts from leaves infiltrated with TRV-BIR1 is shown (right). TRV-GFP and 35S-BIR1-HA were used as controls. Ponceau staining was used as a protein loading control. **(b)** Morphological phenotypes of plants mock-inoculated,

systemically infected with TRV-GFP or infected with TRV-BIR1 WT (referred to as #1 to #6). Plants were grown on soil and photographed at 14 dpi. Percentage of plants displaying normal vs morphological phenotypes after inoculation with TRV-derivatives is indicated. Non-inoculated (healthy) and mock-inoculated plants were used as controls. TRV-GFP was used as control. **(c)** Accumulation of *BIR1* transcripts in TRV-BIR1-infected individual plants shown in (b). Samples from non-inoculated (healthy), mock-inoculated or TRV-GFP-infected plants were included as controls. **(d)** Accumulation of defense-related *PR1* and *PR4* transcripts in TRV-BIR1-infected individual plants shown in (b). TRV-GFP was used as control. **(e)** Accumulation of TRV genomic RNA in TRV-BIR1-infected individual plants shown in (b). Relative expression levels were determined by qRT-PCR and normalized to the *CBP20* internal control. Error bars represent SD from three independent PCR measurements. Asterisks (Student's *t* test) or different letters (one-way ANOVA) were used to indicate significant differences ($P < 0.001$). The experiments were repeated at least three times with similar results and one representative biological replicate is shown.

Figure 7. Phenotypes of *BIR1* overexpressing transgenic Arabidopsis. **(a)** Morphological phenotypes of *BIR1* transgenic plants after DEX treatment. Arabidopsis plants from transgenic line 6 (BIR1 WT L6) were grown for three weeks on soil and treated with 30 μ M DEX or mock-treated for 6 consecutive days by spraying the solution (1 ml per plant) once at 24 h intervals. DEX-treated wild type (Col-0) plants are shown as controls. Plants were photographed at 7 days after the first DEX application. Morphological phenotypes of plants from transgenic line 9 (L9) are shown in Supporting Information Fig. S8(a). **(b)** Accumulation of *BIR1* transcripts in plants from *BIR1* overexpressor lines L6 and L9. Wild type plants are shown as controls. Plants were sprayed with DEX (+) or water (-). Plants showing wild type (-) or aberrant (+) phenotypes were analyzed. **(c)** Western blot analysis of BIR1 proteins in extracts from leaves of lines L6 and L9. Plants were sprayed with DEX (+) or water (-). Plants showing wild type (-) or aberrant (+) phenotypes were analyzed. Ponceau staining was used as a protein loading control. **(d)** Accumulation of defense-related *PR1*, *PR4*, and *PAD3* transcripts in plants from lines L6 and L9. **(e)** Trypan blue staining of leaves of wild type and *BIR1* overexpression lines (L6 and L9). Leaves from DEX-treated and mock-treated plants grown on soil were stained with lactophenol trypan blue as described (Diaz-Tielas *et al.*, 2012). Relative expression levels were determined by qRT-PCR and normalized to the *CBP20* internal control. Error bars represent SD from three independent PCR

measurements. Different letters indicate significant differences according to one-way ANOVA and Duncan test ($P < 0.001$). The experiments were repeated at least three times with similar results and one representative biological replicate is shown.

Author Manuscript



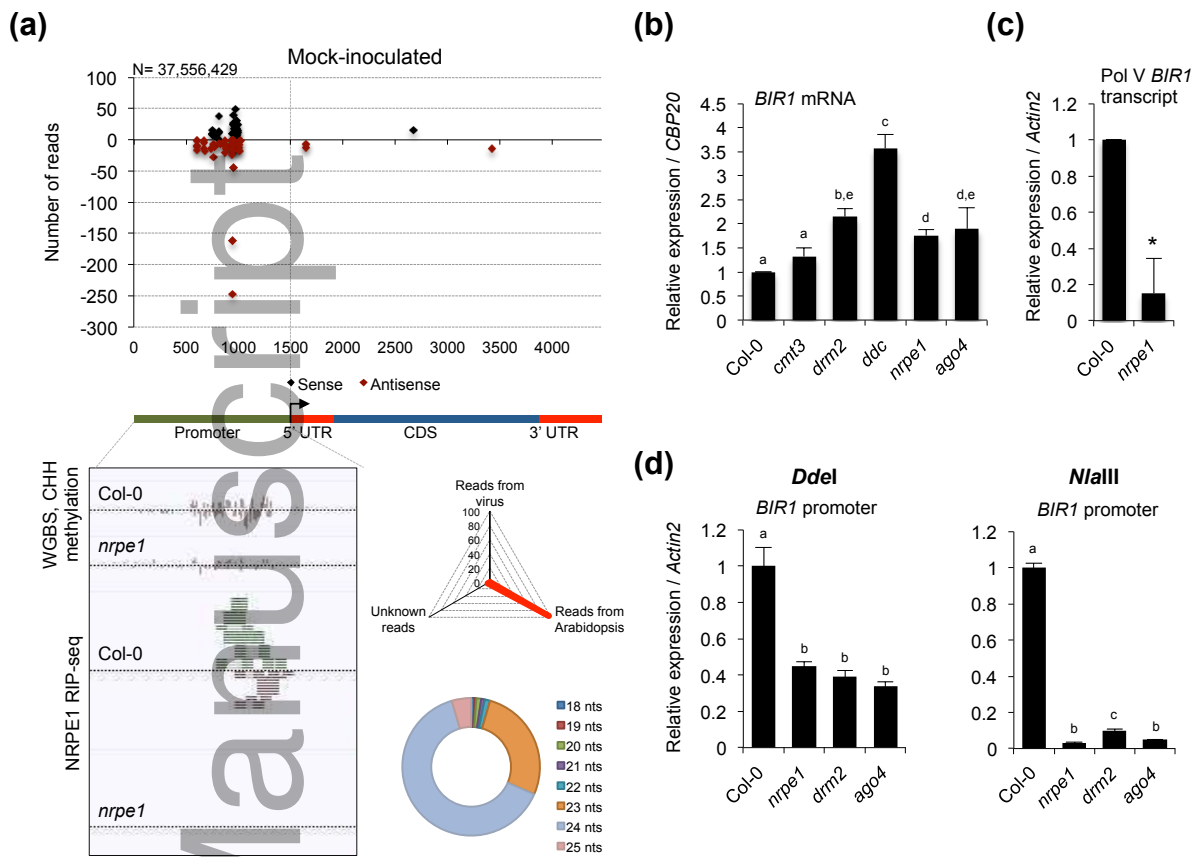
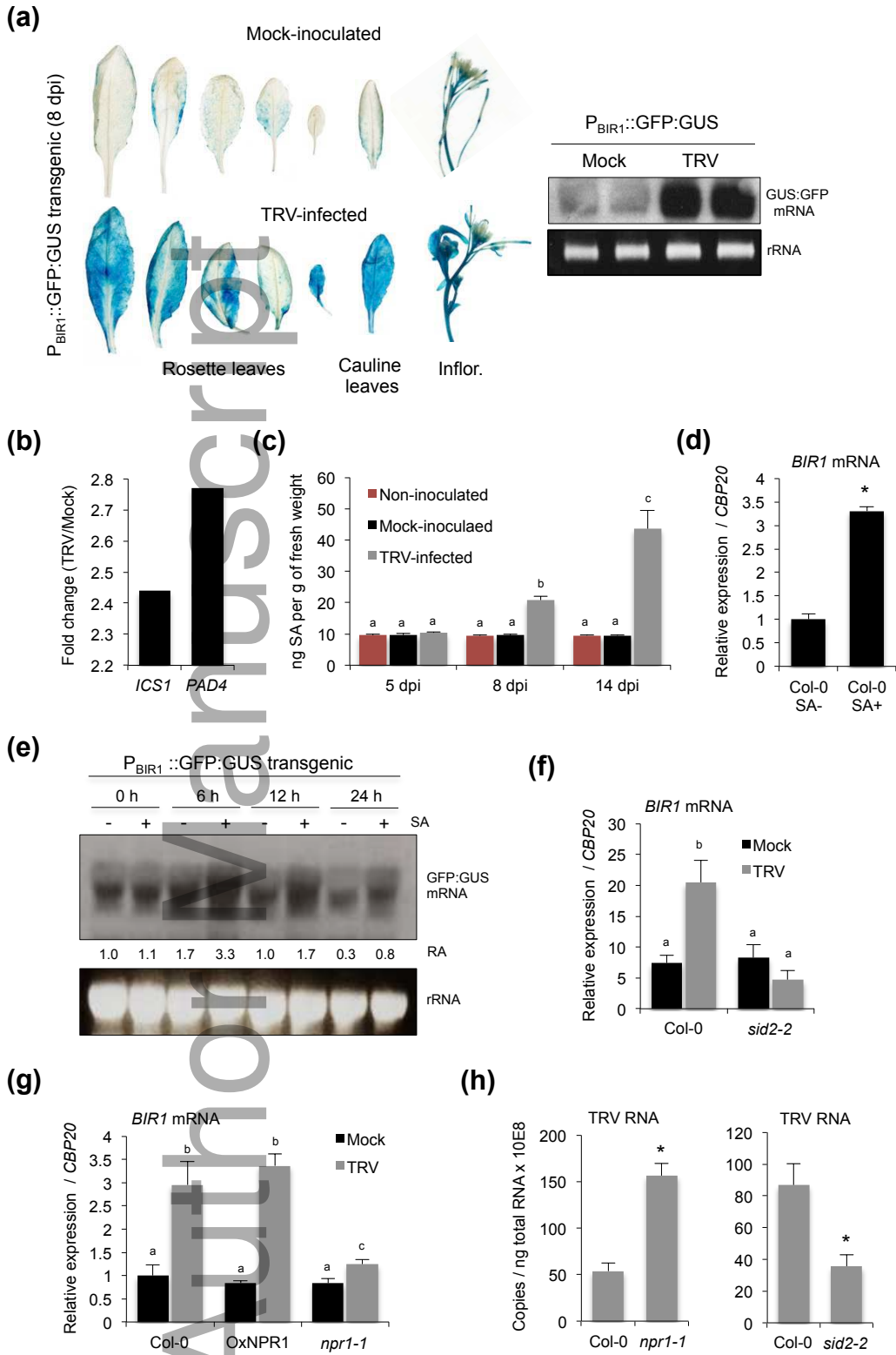


Fig. 2



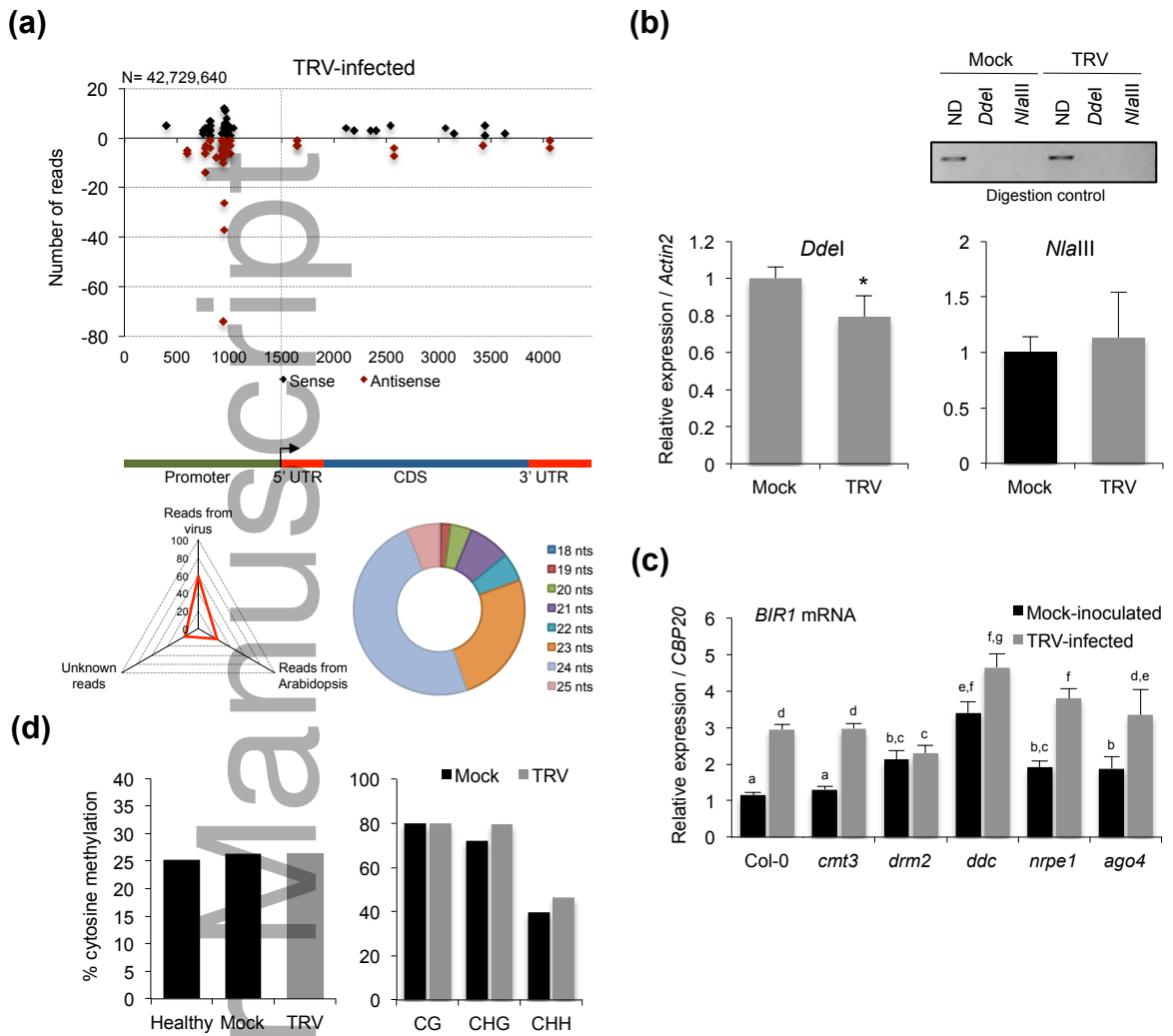


Fig. 4

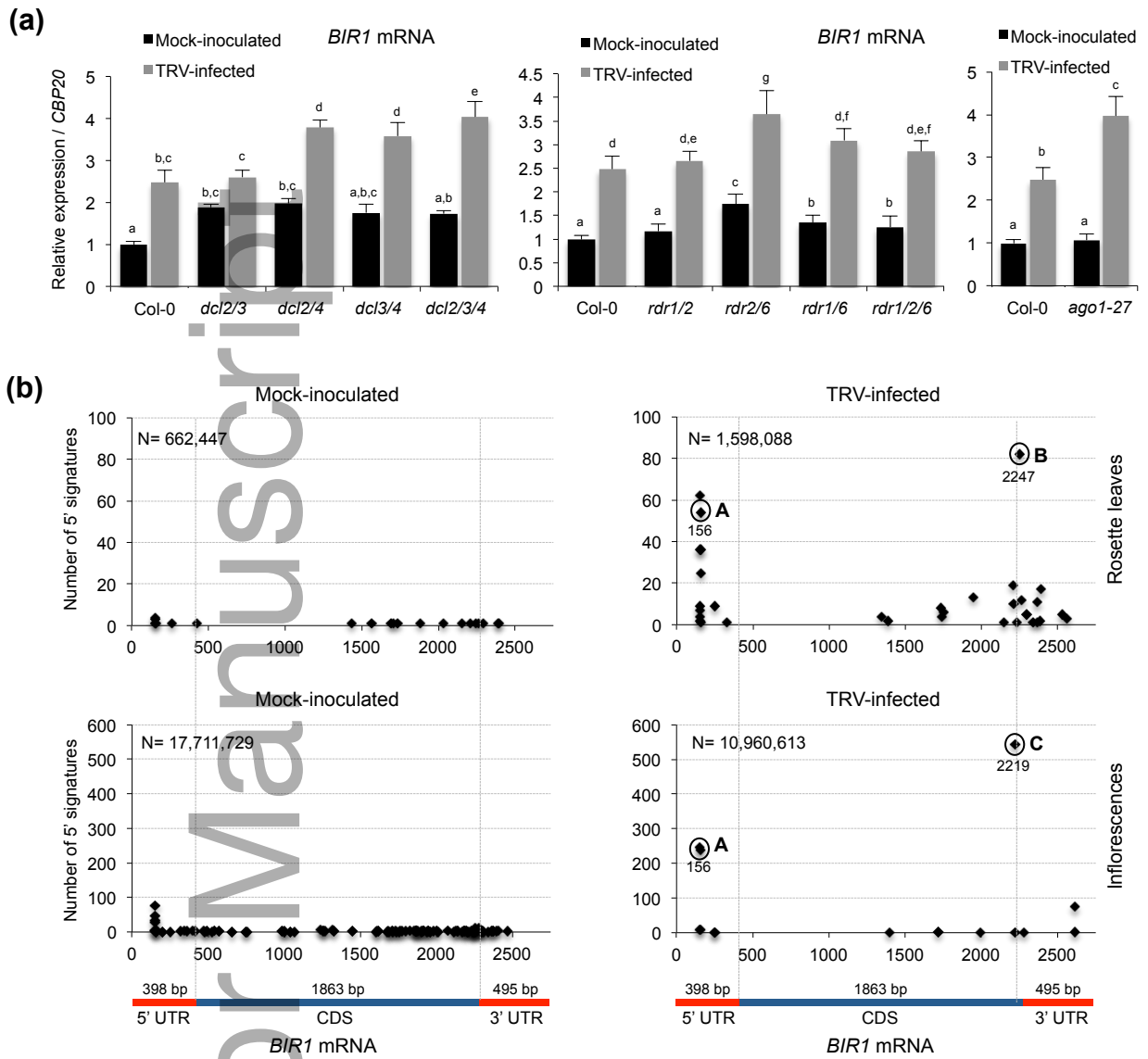


Fig. 5

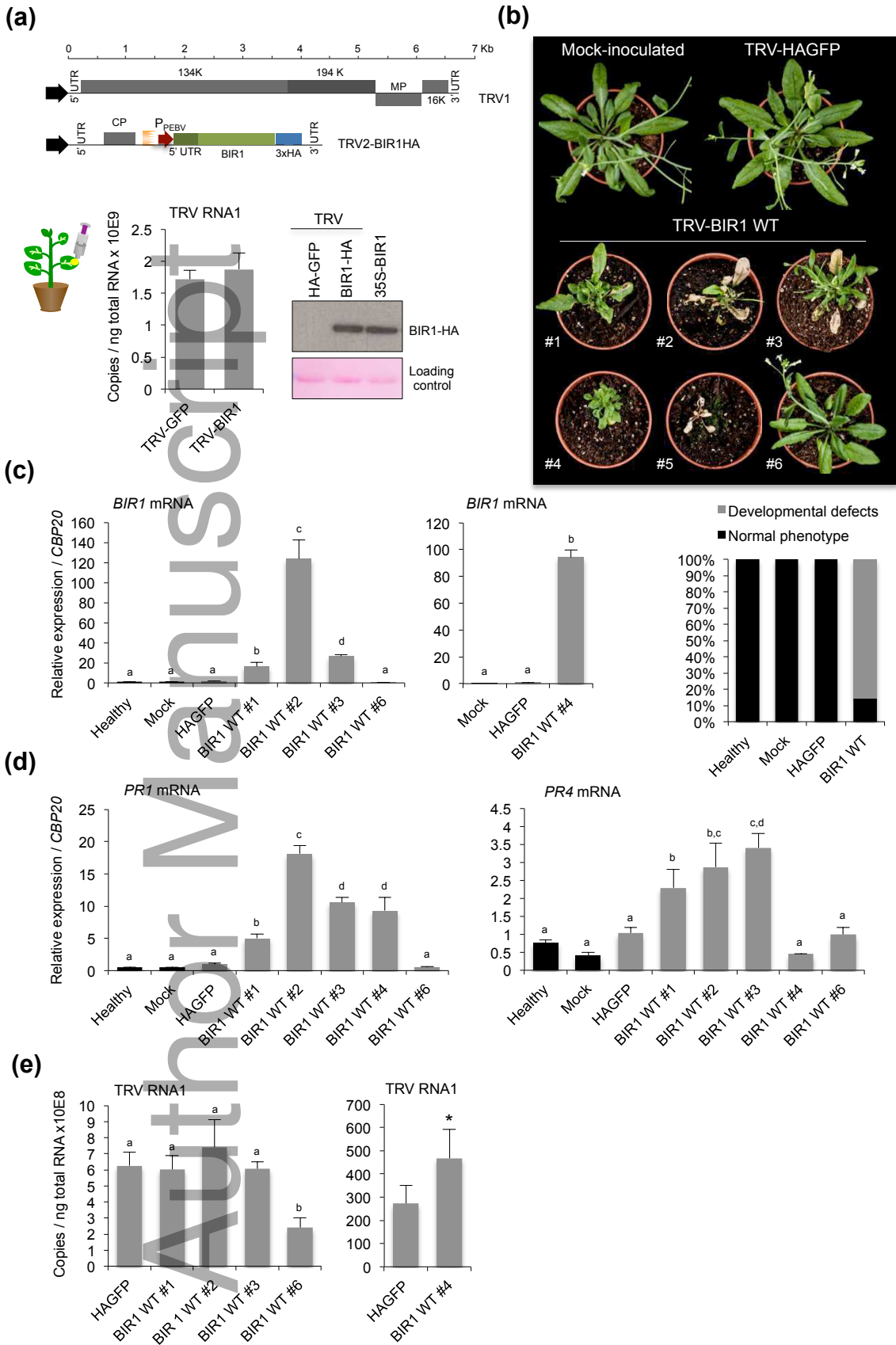
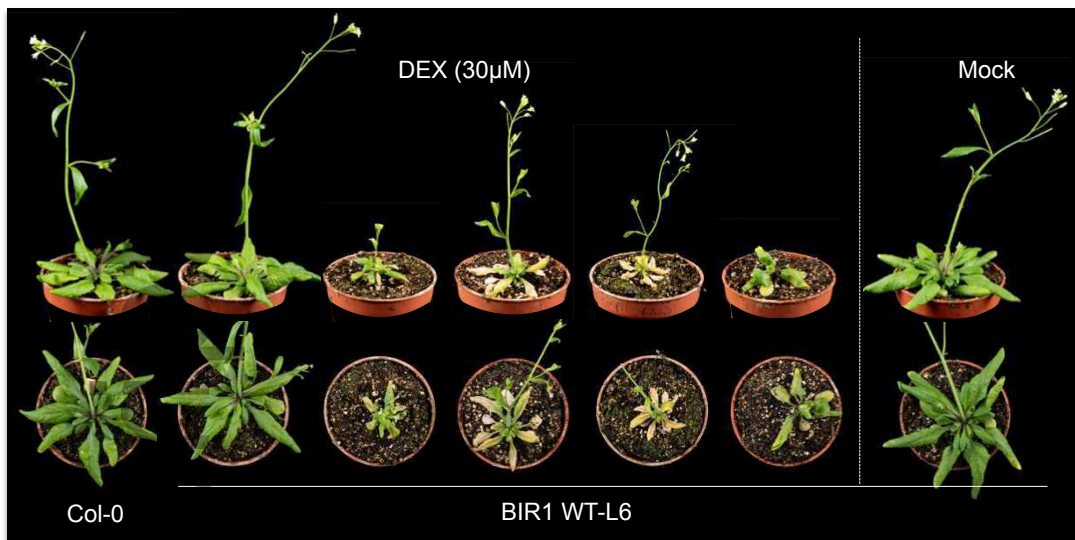
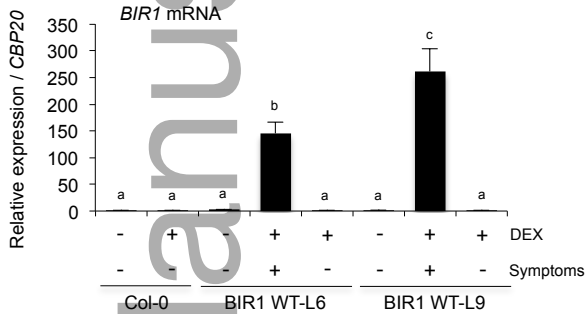


Fig. 6

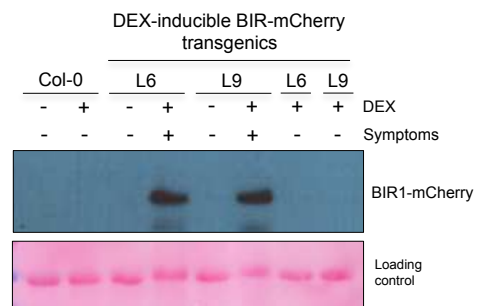
(a)



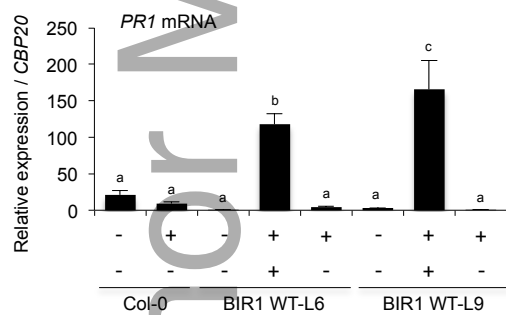
(b)



(c)



(d)



(e)

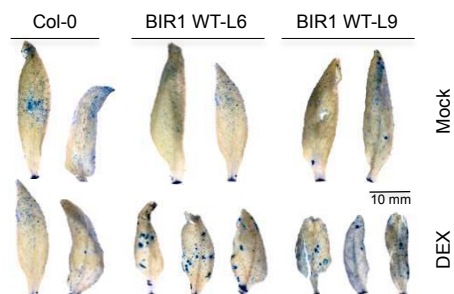
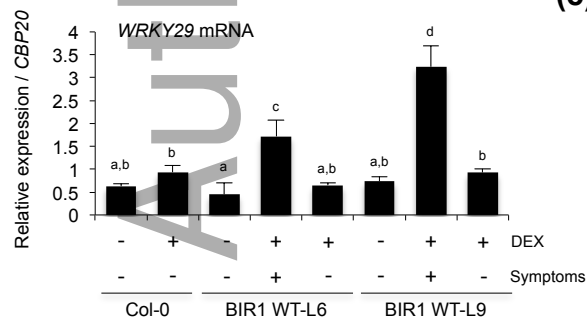


Fig. 7

This article is protected by copyright. All rights reserved